# Spectral, Kinetic, and Theoretical Studies of Sulfur-Centered Reactive Intermediates Derived from Thioethers Containing an Acetyl Group

**Nicolas Varmenot,[†] Jacqueline Bergès,[†,‡] Zohreh Abedinzadeh,*[,†] Anthony Scemama,[‡] Grazyna Strzelczak,[§] and Krzysztof Bobrowski[§]**

*Laboratoire de Chimie Physique, UMR 8601 CNRS, Université René Descartes, 45 rue des Saints-Peres, 75270 Paris Cedex 06, France, Laboratoire de Chimie Theorique, UMR 7616 CNRS, Université P. et M. Curie, 4 place Jussieu 75230, Paris Cedex, France, and Institute of Nuclear Chemistry and Technology, Dorodna 16, 03-195 Warsaw, Poland*

*Received: October 13, 2003; In Final Form: May 3, 2004*

The mechanism of the •OH-induced oxidation of *S*-ethylthioacetate (SETAc) and *S*-ethylthioacetone (SETA) was investigated in aqueous solution using pulse radiolysis and steady-state $\gamma$ radiolysis combined with chromatographic and ESR techniques. For each compound, •OH radicals were added, as an initial step, to the sulfur moiety, forming hydroxysulfuranyl radicals. Their subsequent decomposition strongly depended on the availability of α- or $\beta$-positioned acetyl groups, pH, and the thioether concentration. For SETAc, which contains the α-positioned acetyl group, hydroxysulfuranyl radicals SETAc(>•S−OH) subsequently decay into secondary products, which do not include intermolecularly three-electron-bonded dimeric radical cations, even at high concentrations of SETAc. At low pH, these observations are rationalized in terms of the highly unstable nature of sulfur monomeric radical cations SETAc(>$S^{+\bullet}$) because of their rapid conversion via deprotonation to the α-(alkylthio)alkyl radicals $H_3C-{}^{\bullet}CH-S-C(=O)-CH_3$ ($\lambda_{max}$ = 420 nm). However, at low proton concentrations, the α-positioned acetyl group destabilizes SETAc(>•S−OH) radicals within a five-membered structure that leads to the formation of alkyl-substituted radicals, $H_3C-CH_2-S-C(=O)-{}^{\bullet}CH_2$. A somewhat different picture is observed for SETA, which contains a $\beta$-positioned acetyl group. The main pathway involves the formation of hydroxysulfuranyl radicals SETA(>•S−OH) and α-(alkylthio)alkyl radicals $H_3C-CH_2-S-{}^{\bullet}CH-C(=O)-CH_3$ ($\lambda_{max}$ = 380 nm). The latter radicals are highly stabilized through the combined effect of both substituents in terms of the captodative effect. At low pH, SETA(>•S−OH) radicals undergo efficient conversion to intermolecularly three-electron-bonded dimeric radical cations SETA-(>S∴S<)$^+$ ($\lambda_{max}$ = 500 nm), especially for high SETA concentrations. In contrast, at low proton concentrations, SETA(>•S−OH) radicals decompose via the elimination of water, formed through intramolecular hydrogen transfer within a six-membered structure that leads to the formation of alkyl-substituted radicals, $H_3C-CH_2-S-CH_2-C(=O)-{}^{\bullet}CH_2$. The latter radicals undergo a 1,3-hydrogen shift and intramolecular hydrogen abstraction within the six-membered structure, leading to the α-(alkylthio)alkyl radicals $H_3C-CH_2-S-{}^{\bullet}CH-C(=O)-CH_3$ and $H_3C-{}^{\bullet}CH-S-CH_2-C(=O)-CH_3$, respectively. To support our conclusions, quantum mechanical calculations were performed using density functional theory (DFT-B3LYP) and second-order Møller−Plesset perturbation theory (MP2) to calculate the bond-formation energies of some key transients and the location and strength of their associated optical absorptions.

## Introduction

Neighboring groups appear to have a major influence on the course of oxidative attack of organic sulfur compounds.[1,2] In general, neighboring groups act catalytically through transient bond formation between sulfur radical cationic intermediates and functional groups carrying electron lone pairs.[1,3−6] This is illustrated by the large variety of products following the oxidation of multifunctional thioethers by hydroxyl radicals.[7−28] These results are important for unraveling analogous mechanisms in biological systems that are exposed to oxidative stress.[29,30] The fate of the reactive species formed by an initial attack at a sulfur atom is of interest in following the course of the reaction to the ultimate damage site and in understanding possible repair mechanisms.[31,32] In addition, there are pharmaceutical applications that could benefit from an understanding of how oxidative processes destabilize formulations of peptides and protein-based drugs.[33]

Recently,[34] detailed studies of *N*,*S*-diacetyl-L-cysteine ethyl ester (SNACET) showed that the adjacent electron-withdrawing acetyl group destabilizes hydroxysulfuranyl radicals because of a very fast fragmentation into acyl radicals and the respective sulfenic acid. In contrast, the monomeric radical cations are stabilized by the adjacent acetyl group because of spin delocalization onto the carbonyl group. In a continuation of our work on the effect of the electron-withdrawing functional group (acetyl group, $H_3C-C=O$) on the stability of the hydroxysulfuranyl radicals and the sulfur radical cationic interemediates,

* Corresponding author. Fax: +33−1−42 86 83 87. E-mail: abedinzadeh@biomedicale.univ-paris5.fr.
[†] Université René Descartes.
[‡] Université P. et M. Curie.
[§] Institute of Nuclear Chemistry and Technology.

10.1021/jp031159b CCC: $27.50 
Published on Web 07/02/2004

we have extended our studies to the reactions of the •OH radicals with two model thioether compounds, *S*-ethylthioacetate and *S*-ethylthioacetone, containing acetyl groups in the α and $\beta$ positions with respect to the sulfur atom, respectively.

Furthermore, to support our conclusions, we performed quantum mechanical ab initio calculations by using density functional theory (DFT-B3LYP) and second-order Møller−Plesset perturbation theory (MP2) to calculate the bond formation energies of some of the key transients and the location and strength of their associated optical absorptions.

## Experimental Section

**Materials.** *S*-Ethylthioacetate (SETAc) ($H_3C-CH_2-S-CO-CH_3$) and *S*-ethylthioacetone (SETA) ($H_3C-CH_2-S-CH_2-CO-CH_3$) were purchased from Lancaster (Pelham, NH). All chemicals were of the purest commercially available grade and were used as received. Potassium peroxydisulfate ($K_2S_2O_8$) was from the Sigma Chemical Company (St. Louis, MO). Solutions were made with deionized water (18-MΩ resistance) provided by a Millipore Milli-Q system. The pH was adjusted by the addition of either NaOH or $HClO_4$. Solutions were subsequently purged for at least 30 min per 500-mL sample with the desired gas ($N_2O$, $N_2$, or $O_2$) before pulse irradiation and for 15 min per 5-mL sample with $N_2O$ before $\gamma$ irradiation. To establish whether S-ethylthioacetate hydrolyzes or fragments to the ketene and thiol,[35] we checked $N_2O$-saturated aqueous solutions containing $10^{-3}$ M SETAc at pH 1 and 6 for the presence of thiols. The concentration of thiols was determined by Ellman's reagent (5,5′-dithiobis(2-nitrobenzoic acid)),[36] which undergoes a thiolate−disulfide exchange reaction to yield 2-nitromercaptobenzoic acid. This reaction was followed spectrophotometrically at $\lambda = 412$ nm with $\epsilon_{412} = 13\,600$ $M^{-1}$ $cm^{-1}$. No presence of thiols was observed in SETAc solutions a few hours after dissolution.

**Pulse Radiolysis.** Pulse-radiolysis experiments were performed with 5−17-ns pulses of 6-MeV electrons from the Lodz Technical University ELU-6 linear accelerator.[37,38] The absorbed doses were on the order of 8−15 Gy (1 Gy = 1 J $kg^{-1}$). Signal averaging methods were used. A description of the pulse-radiolysis setup and data collection has been reported elsewhere. The $N_2O$-saturated $10^{-2}$ M solutions of potassium thiocyanate were used as the dosimeter, taking a radiation chemical yield of 6.13 and a molar extinction coefficient of 7580 $M^{-1}$ $cm^{-1}$ at 472 nm.[39] All experiments were carried out with continuously flowing solutions.

**Electron Spin Resonance.** Electron spin resonance (ESR) experiments were performed using a Bruker-ESP300 spectrometer operating in the X band (9.5 GHz) equipped with a cryostat and a variable temperature unit over the temperature range of 77−293 K. The degassed samples of frozen *S*-ethylthioacetate and *S*-ethylthioacetone were irradiated in spectrosil tubes (immersed in liquid nitrogen) with doses of about 5 kGy from a $^{60}Co$ $\gamma$ source (Issledovatel, USSR) at the Institute of Nuclear Chemistry and Technology, Warsaw. The measurements were performed either in vacuum or in the presence of oxygen. The ESR spectra were analyzed by computer simulations using EPR software provided by Dr. D. L. Dulling from the NIEHS LMB National Institute of Health.

**Analysis of Stable Products.** Acetaldehyde was analyzed on the basis of the derivatization technique with PFBOA [*O*-(2,3,4,5,6-pentaflurobenzyl)-hydroxylamine].[40] An aliquot of an irradiated solution was acidified to pH 2 and derivatized by the addition of PFBOA by heating the sample at 45 °C for 2h. Subsequently, the reaction mixture was cooled to room temperature, extracted with 2-heptanol, and injected into a GC column.

The identification and detection of carbon monoxide (CO) was performed by the carbon monoxide/hemoglobin complexometry method.[41] Ferrous hemoglobin (64.5 kDa) reacts stoichiometrically with CO to form the carbon monoxide derivative that exhibits a very sharp Soret band at $\lambda = 419$ nm with an extinction coefficient of $\epsilon_{419} = 1.91 \times 10^4$ $M^{-1}$ $cm^{-1}$. The lowest detection level is typically 1 $\mu$M. $\gamma$ irradiations were performed with an IBL 637 irradiator composed of a $^{137}Cs$ source (222 Tbq, Institut Curie, Paris) using a dose rate of 9.8 Gy $min^{-1}$. UV−vis absorption spectra were recorded using a Beckman DU 70 spectrophotometer.

**Computational Details.** Two ab initio methods were used for the calculations. The first one is the hybrid functional of DFT, the B3LYP method, which is paricularly cost effective and commonly used for localized radical structures.[42] The second one is the Møller−Plesset perturbation method at the MP2 level used for some domains of application for which the accuracy of DFT approximations has not been established, especially for systems with two-center−three-electron (2c, 3e) bonding.[43−45] All geometries were optimized using a gradient technique. The calculations were performed with the standard 6-31G* for the B3LYP method. The use of this relatively small basis set is justified by the number of geometry optimizations and by the fact that DFT methods are known to be weakly dependent on basis sets.[46] Errors resulting from basis-set dependence are more significant for the (2c, 3e) systems. However, it was shown[47] that the 6-31+G* basis was accurate for the OH adduct to sulfur in dimethyl sulfide and led to similar binding energies obtained by MP2 and more sophisticated quadratic-configuration interaction including single, double, and triple substitution QCISD(T) calculations. All calculations on radical species using DFT or MP methods were performed within the spin-unrestricted formalism. The zero-point energy (ZPE) corrections were found to be relatively small for all species except for the OH adducts. The influence of solvent on neutral radicals and radical ions was taken into account by adopting polarized continuum models (PCM).[48−50] These models are only rough estimations;[51] nevertheless, they can be useful for analyzing tendencies. The geometries of solvated species were reoptimized by the B3LYP method but not with the MP2 method.

The calculations of optical absorption peaks together with dipole oscillator strengths were carried out with two methods: B3LYP/6-31G* and the density functional B3PW91 with the extended basis set, cc-pVTZ (Dunning's triple zeta correlation-consistent basis sets). These are well adapted for the calculation of spectra within time-dependent density functional theory (TD-DFT).[52] However, there are two limits to these calculations: the electronic transitions concerned are vertical, and solvent effects are not included.

All calculations were performed with the Gaussian 98 quantum chemistry program[53] with the COSMO option for the conductor polarized continuum model (CPCM) method.

## Results

**Radiolysis of Water.** The radiolysis of water leads to the formation of the primary reactive species shown in reaction 1. In $N_2O$-saturated solutions ($[N_2O]_{sat} \approx 2 \times 10^{-2}$ M), the hydrated electrons, $e_{aq}^-$, are converted into •OH radicals according to eq 2 ($k_2 = 9.1 \times 10^9$ $M^{-1}$ $s^{-1}$). Reaction 2 nearly

doubles the number of •OH radicals available for reaction with substrates.

$$H_2O \rightarrow {}^{\bullet}OH,\ e_{aq}^{-},\ {}^{\bullet}H \quad (1)$$

$$e_{aq}^{-} + N_2O + H_2O \rightarrow {}^{\bullet}OH + OH^{-} + N_2 \quad (2)$$

The effective radiation chemical yields, $G$, of the primary species available for reaction with a substrate depend on the concentration of the added substrate. For $N_2O$-saturated solutions, the effective radiation chemical yield of •OH radicals converting a given substrate into substrate-derived radicals can be calculated on the basis of the equation given by Schuler et al.[54] This equation relates the $G$ value of substrate radicals to the product of the rate constant for the reaction of the •OH radicals with the substrate and the substrate concentration. At pH < 4, the diffusion-controlled reaction of $e_{aq}^{-}$ with protons becomes important (reaction 3, $k_3 = 2.0 \times 10^{10}$ $M^{-1}$ $s^{-1}$)

$$e_{aq}^{-} + H^{+} \rightarrow {}^{\bullet}H \quad (3)$$

resulting in a pH-dependent lowered yield of •OH radicals and a corresponding increased yield of •H atoms. For the selective monitoring of the reaction of •OH radicals with a substrate at very low pH, the solution was saturated with oxygen. Under these conditions, •H atoms are rapidly converted into perhydroxyl radicals according to eq 4 ($k_4 = 2.1 \times 10^{10}$ $M^{-1}$ $s^{-1}$).

$$ {}^{\bullet}H + O_2 \rightarrow {}^{\bullet}HO_2 \quad (4)$$

To study the reaction between •H atoms and a substrate, we acidified the solutions to pH 1 and added 0.5 M 2-methyl-2-propanol (*t*-BuOH) to the solution to scavenge the •OH radicals (reaction 5, $k_5 = 6.8 \times 10^{8}$ $M^{-1}$ $s^{-1}$)

$$ {}^{\bullet}OH + (CH_3)_3COH \rightarrow {}^{\bullet}CH_2(CH_3)_2{-}COH + H_2O \quad (5)$$

Sulfate radical anions ($SO_4^{\bullet-}$) were also used as oxidizing species to convert a substrate into the corresponding radical cations. The $SO_4^{\bullet-}$ radical anions were produced in Ar-saturated solutions containing $S_2O_8^{2-}$ and *tert*-butyl alcohol at pH 5.5−6.0. Under these conditions, the $SO_4^{\bullet-}$ radical anions are formed according to eq 6 ($k_6 = 1.2 \times 10^{10}$ $M^{-1}$ $s^{-1}$).

$$e_{aq}^{-} + S_2O_8^{2-} \rightarrow SO_4^{\bullet-} + SO_4^{2-} \quad (6)$$

•OH radicals do not interfere with the measurement because of reaction 5.

***S*-Ethylthioacetate (SETAc).** With respect to the sulfur atom, SETAc contains an α-positioned acetyl group. The reaction of •OH radicals with SETAc was investigated in $N_2O$-saturated solutions over the concentration range of $2 \times 10^{-4}$−$5 \times 10^{-2}$ M in the pH range of 1−6.

**Mechanistic Studies with the Hydroxyl Radical.** *Influence of pH.* Depending on the pH, pulse irradiation leads to different transient optical spectra. A broad absorption band, 90 ns after pulse irradiation of an $N_2O$-saturated aqueous solution, pH 1, containing $10^{-3}$ M SETAc, was observed in the 260−500 nm range with $\lambda_{max} = 280$ nm and a pronounced shoulder around 300−400 nm (Figure 1A, curve a).

A part of the pronounced absorption shoulder is short lived and decays within 0.5 μs after the pulse, as measured at $\lambda = 350$ nm (middle right inset in Figure 1A). A resulting absorption spectrum after 280 ns is characterized by two distinct absorption maxima at $\lambda_{max} = 280$ and 420 nm, with the respective $G \times \epsilon = 10\,900$ and 3650 $M^{-1}$ $cm^{-1}$ (Figure 1A, curve b). At longer times (10, 50, and 100 μs after the pulse), the intensity of both 280- and 420-nm bands decreases; however, the 420-nm band decays faster (Figure 1A, curves c, d, and e). The strong absorption band with $\lambda_{max} = 280$ nm indicates the presence of α-(alkylthio)alkyl-type radicals. It may be anticipated (and is supported by theoretical calculations, vide infra) that one of the most stable α-(alkylthio)alkyl radicals is $H_3C{-}{}^{\bullet}CH{-}S{-}CO{-}CH_3$, which can be formed via direct hydrogen abstraction from the adjacent methylene group (reaction 7)

$$ {}^{\bullet}OH + H_3C{-}CH_2{-}S{-}CO{-}CH_3 \rightarrow H_3C{-}{}^{\bullet}CH{-}S{-}CO{-}CH_3 + H_2O \quad (7)$$

or via deprotonation of the monomeric sulfur radical cation (SETAc)>$S^{\bullet+}$ in reaction 8.

$$H_3C{-}CH_2{-}S^{\bullet+}{-}CO{-}CH_3 \rightarrow H_3C{-}{}^{\bullet}CH{-}S{-}CO{-}CH_3 + H^{+} \quad (8)$$

To study the pH dependence of the formation of the 420-nm species, we performed pulse-radiolysis experiments in $N_2O$-saturated aqueous solutions containing $10^{-3}$ M SETAc at different pH values over the range of 1−6. The yield of the 420-nm species (normalized to the actual yield of the •OH radical concentration taking into account the variation with pH) was found to decrease with increasing pH (top left inset in Figure 1A) in similar way to that which occurs in SNACET solutions. However, the plot of the normalized $G \times \epsilon_{420}$ ($G_{rel}$), which takes a sigmoidal shape down to about pH 4, is characterized by the inflection point at pH 3.3. The value is shifted by more than 1 pH unit to a higher pH compared to the inflection point observed in SNACET solutions.[34] Moreover, the normalized $G \times \epsilon_{420}$ ($G_{rel}$) yields measured on the plateau between pH 4 and 6 account for ca. 40% of the normalized $G \times \epsilon_{420}$ ($G_{rel}$) yield measured at pH 1. The last observation also differs from that found in SNACET solutions where the normalized $G \times \epsilon_{420}$ ($G_{rel}$) yields measured on the plateau between pH 3.5 and 6 account for less than 5% of the normalized $G \times \epsilon_{420}$ ($G_{rel}$) yield measured at pH 1.[34] The 420-nm species is long lived, and its lifetime is substantially enhanced ($t_{1/2} \approx 50$ μs) (bottom right inset in Figure 1A) compared to the lifetime of the monomeric sulfur radical cation (SNACET>$S^{\bullet+}$) ($t_{1/2} \approx 2.5$ μs) measured at the same pH and concentration conditions.[34] Therefore, at this point of the exposition, some doubts arise as to whether the 420-nm absorption band can be assigned to (SETAc)>$S^{\bullet+}$.

*Influence of Concentration.* To determine whether the 420-nm absorption band can be assigned to either the monomeric sulfur radical cation (>$S^{\bullet+}$) or the intermolecular dimeric three-electron-bonded sulfur radical cation (>S∴S<)$^{+}$ derived from SETAc, we performed pulse-radiolysis experiments with various concentrations, $10^{-3}$−$5 \times 10^{-2}$ M, of SETAc. Solutions of pH 1 were used to ensure a high concentration of protons to promote the elimination of water and the fast formation of a monomeric sulfur radical cation, (SETAc)>$S^{\bullet+}$, according to reactions 9 and 10:

$$ {}^{\bullet}OH + H_3C{-}CH_2{-}S{-}CO{-}CH_3 \rightarrow H_3C{-}CH_2{-}S^{\bullet}(OH){-}CO{-}CH_3 \quad (9)$$

$$H_3C{-}CH_2{-}S^{\bullet}(OH){-}CO{-}CH_3 + H^{+} \rightarrow H_3C{-}CH_2{-}S^{\bullet+}{-}CO{-}CH_3 + H_2O \quad (10)$$

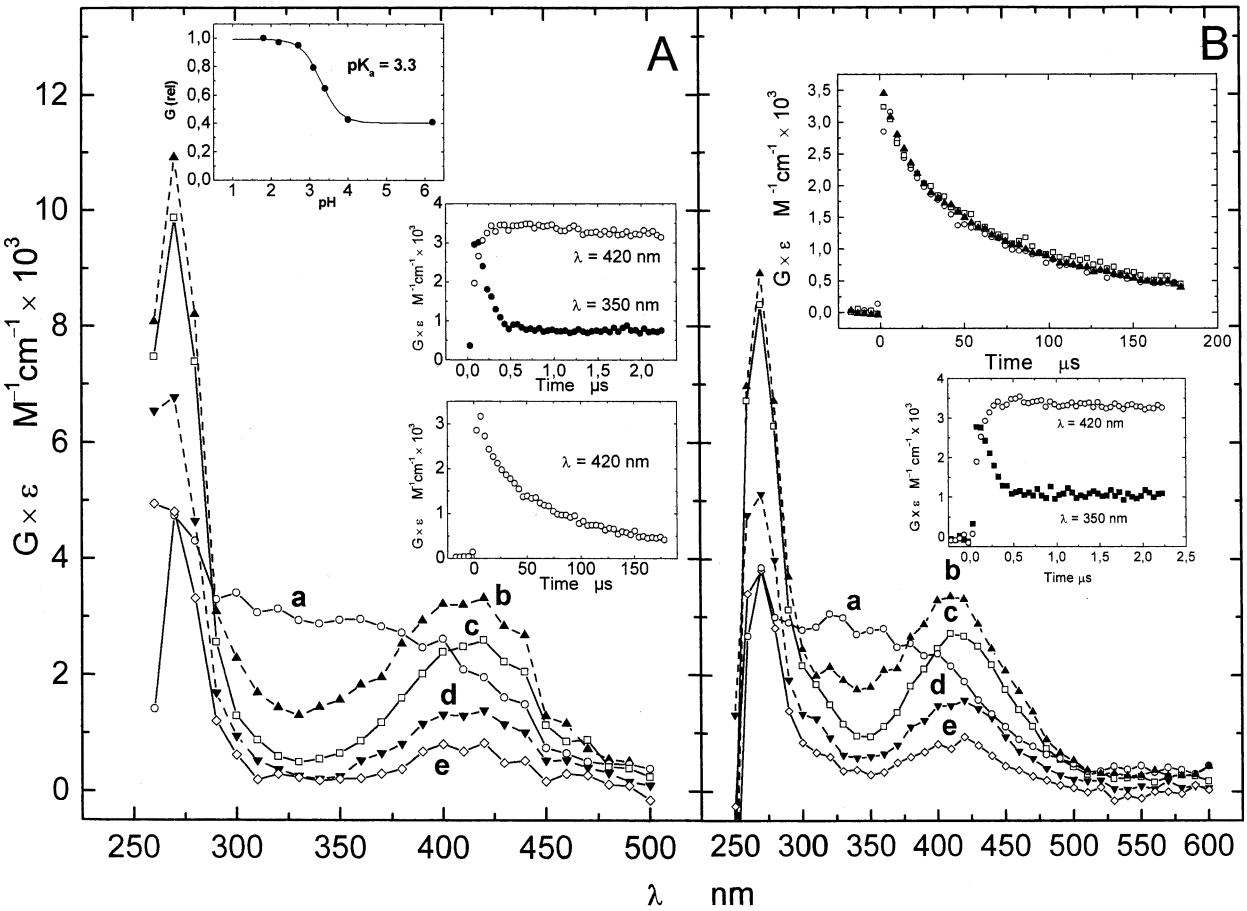


**Figure 1.** (A) Transient absorption spectra observed in $N_2O$-saturated aqueous solution at pH 1 containing $10^{-3}$ M *S*-ethylthioacetate (SETAc) (○) 90 ns, (▲) 280 ns, (□) 10 $\mu$s, (▼) 50 $\mu$s, and (◇) 100 $\mu$s after pulse irradiation. Insets: (top left) plot of the $G \times \epsilon_{420}$ of the 420-nm species (normalized to the actual •OH radical concentration) as a function of pH; (top right): kinetic traces for a decay of the 350-nm and a formation of the 420-nm absorbances; (bottom right): kinetic trace for decay of the 420-nm absorbance. (B) Transient absorption spectra observed in $N_2O$-saturated aqueous solution at pH 1 containing $5 \times 10^{-2}$ M *S*-ethylthioacetate (SETAc) (○) 90 ns, (▲) 280 ns, (□) 10 $\mu$s, (▼) 50 $\mu$s, and (◇) 100 $\mu$s after pulse irradiation. Insets: (top) kinetic traces for decays of the 420-nm absorbance for different concentrations of *S*-ethylthioacetate (SETAc): (○) $10^{-3}$ M, (▲) $10^{-2}$ M, (□) $5 \times 10^{-2}$ M; (bottom) kinetic traces for a decay of the 350-nm and a formation of the 420-nm absorbances.

However, the high concentration of SETAc should facilitate the formation of the dimeric sulfur radical cation, (SETAc)(S∴S)$^+$, if any, according to reaction 11:

$$(\text{SETAc})\text{>}S^{\bullet+} + \text{SETAc} \rightarrow (\text{SETAc})(\text{S}\therefore\text{S})^+ \qquad (11)$$

It can be seen from Table 1S (Supporting Information) that the radiation chemical yields, expressed as $G \times \epsilon_{420}$, were found in the range of 3500−3800 $M^{-1}cm^{-1}$. Moreover, they increase by only ∼10% with increasing SETAc concentration, that is, in a similar way to the *G* values of •OH radicals that are available to react with SETAc (calculated on the basis of the equation given by Schuler et al.).[54]

We note that the intensities of the 420-nm absorption band, expressed as $G \times \epsilon_{420}$, are ∼2.5-fold lower than the respective intensities of the 420-nm absorption band measured for similar concentrations in SNACET solutions.[34] This means that either the formation of the respective monomeric radical cations (>S$^{\bullet+}$) in SETAc and SNACET solutions does not occur with the same chemical radiation yield or the absorption band with a maximum located at $\lambda_{max} = 420$ nm observed in aqueous solutions containing SETAc has to be assigned to another species. (See Discussion.)

Moreover, a detailed kinetic analysis of the decay of the 420-nm absorption band shows that its half-life does not change at all with SETAc concentration (Figure 1B, top inset). The first-order rate constants determined at various concentrations of SETAc give the same value of $k_d^{420} = 2 \times 10^4$ s$^{-1}$. This observation does not resemble kinetic results in SNACET solutions where the 420-nm intermediate decays in a SNACET concentration-dependent process ($k_{S-S} = 2.2 \times 10^7$ M$^{-1}$ s$^{-1}$) and in a SNACET concentration-independent process ($k_d = 2.5 \times 10^5$ s$^{-1}$). Thus, the value of $k_d^{420}$ is more than 1 order of magnitude smaller than the reported value for the first-order decay component of the (SNACET)>S$^{\bullet+}$.

It can be seen in Figure 1B that the transient absorption spectra recorded at pH 1 for the highest concentration of SETAc ($5 \times 10^{-2}$ M) resemble those recorded for the lowest concentration of SETAc ($10^{-3}$ M) (Figure 1A). Again, a broad absorption band was observed in the 260−500-nm range with $\lambda_{max} = 280$ nm and a pronounced shoulder around 300−400 nm 90 ns after pulse irradiation of an $N_2O$-saturated aqueous solution, pH 1, containing $5 \times 10^{-2}$ M SETAc. (Figure 1B, curve a). A part of the pronounced absorption shoulder is short lived and decays within 0.5 $\mu$s after the pulse. This decay is accompanied by a concominant formation of absorption bands at 280 and 420 nm (Figure 1A, middle inset and Figure 1B, inset). A potential candidate responsible for this short-lived absorption might be the monomeric sulfur radical cations of SETAc. The justification for this assumption is that the 350-nm absorption band develops much faster than other absorption bands, that is, the 280- and 420-nm bands. Moreover, its short lifetime is consistent with the calculated unfavorable formation energy of SETAc(>S$^{\bullet+}$)

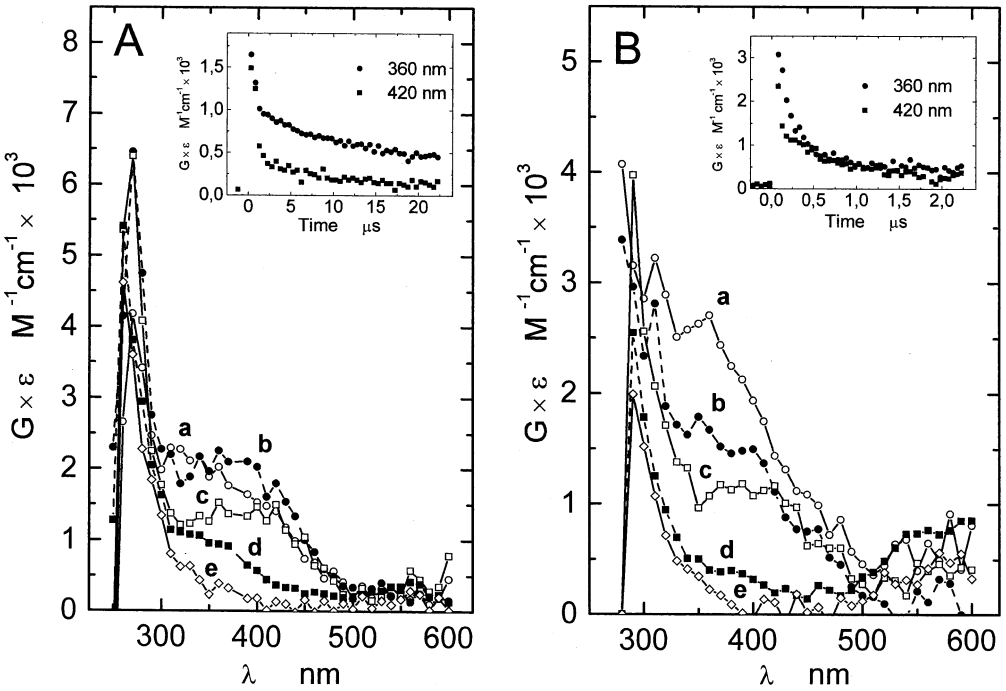


**Figure 2.** (A) Transient absorption spectra observed in $O_2$-saturated aqueous solution at pH 1 containing $10^{-3}$ M *S*-ethylthioacetate (SETAc) (○) 130 ns, (●) 230 ns, (□) 680 ns (■),2.3 $\mu$s, and (◇) 30 $\mu$s after pulse irradiation. Inset: kinetic traces for decays of 360-nm and 420-nm absorbances. (B) Transient absorption spectra observed in $O_2$-saturated aqueous solution at pH 6 containing $5 \times 10^{-3}$ M *S*-ethylthioacetate (SETAc) (○) 130 ns, (●) 230 ns, (□) 380 ns (■) 2.3 $\mu$s, and (◇) 30 $\mu$s after pulse irradiation. Inset: kinetic traces for decays of 360- and 420-nm absorbances.

(vide infra). The decay rate measured at 350 nm ($k_d^{350}$) does not depend on the SETAc concentration because the decay rates ($k_d^{350}$) measured at the lowest ($10^{-3}$ M) and highest ($5 \times 10^{-2}$ M) concentrations of SETAc are similar. We conclude that this decay could be assigned to the first-order process involving the intramolecular transformation of the SETAc($>S^{\bullet+}$) into α-(alkylthio)alkyl-type radicals $H_3C-{}^{\bullet}CH-S-CO-CH_3$ via deprotonation (vide supra, reaction 8). A resulting absorption spectrum after 280 ns is characterized by two distinct absorption maxima at $\lambda_{max} = 280$ and 420 nm, with the respective $G \times \epsilon = 8800$ and 3750 $M^{-1}$ $cm^{-1}$ (Figure 1B, curve b). It is noteworthy that the transient absorption spectra recorded 280 ns after the electron pulse at pH 1 for two extreme concentrations of SETAc (1 and 50 mM) are characterized by two absorption bands: one stronger on the UV side with $\lambda_{max}$ in the neighborhood of 280 nm and the weaker second absorption band with $\lambda_{max} = 420$ nm (Figure 1A and B) with similar radiation chemical yields of $G \times \epsilon_{420} \approx 3500$ $M^{-1}$ $cm^{-1}$.

Because the changes of the absorption spectra with elapsed time were very subtle, for the sake of comparison, all spectra were normalized to the 420-nm absorption maximum. Contrary to the observations in SNACET solutions,[34] there is no buildup of normalized absorption in the regions of $\lambda = 330-390$ nm and 470−500 nm, which was indicative of the existence of the acetyl thiyl radicals in enolic form and intermolecularly three-electron-bonded radical cations, respectively. This observation clearly indicates that the formation of SETAc($>S\therefore S<)^+$ has to be very inefficient over the concentration studied from $10^{-3}$ up to $5 \times 10^{-2}$ M and is compatible with the lack of influence of SETAc concentration on the decay rate of 350-nm absorption. The assignment of 350-nm absorption to SETAc($>S^{\bullet+}$) finds additional support from the experiments in oxygenated systems (vide infra) and theoretical calculations. (See Table 2S in Supporting Information.)

*Influence of Oxygen: Acidic Region.* Upon pulse radiolysis of oxygenated aqueous solutions, pH 1, containing $10^{-3}$ M SETAc, the transient absorption spectrum observed 130 ns after the pulse is characterized by the absorption band with $\lambda_{max} \approx$ 280 nm and a pronounced shoulder around 300−400 nm (Figure 2A, curve a).

A part of the pronounced absorption shoulder is short lived and decays within 0.5 $\mu$s after the pulse as measured at $\lambda =$ 360 nm (inset in Figure 2A). The decay rate of the 360-nm absorption is not affected by the presence of oxygen, confirming a contribution of the cationic radical species to the absorption that is manifested in the absorption shoulder around 300−400 nm. This observation confirms our earlier assignment of the 350-nm absorption band to the sulfur monomeric radical cation of SETAc. With elapsing time, the absorption band with $\lambda_{max} =$ 420 nm becomes more pronounced, and the resulting spectrum recorded 230 ns after the pulse consists of two absorption bands with maxima located at 280 and 420 nm with respective radiation chemical yields of $G \times \epsilon = 6500$ and 2250 $M^{-1}$ $cm^{-1}$ (Figure 2A, curve b). The comparison of the absorption spectra obtained both in $N_2O$- and $O_2$-saturated solutions (Figures 1A, curve b and 2A, curve b) reveals that the intensities of both absorption bands observed at the respective maxima of $\lambda_{max} \approx 280$ and 420 nm, expressed as $G \times \epsilon$, appear to be much lower for $O_2$-saturated solutions, suggesting a contribution mainly of the C-centered radicals to the 280- and 420-nm absorption bands. The 420-nm absorption is even better developed at 680 ns after the pulse (Figure 2A, curve c); however, its intensity is lower as compared with the intensity of the 420-nm absorption observed in $N_2O$-saturated solutions 10 $\mu$s after the pulse (Figure 1A, curve c). A detailed kinetic analysis of the decay of 420-nm absorption shows clearly that its half life decreases with oxygen concentration, as would be expected for the $C^{\bullet}$-centered radicals (inset in Figure 2A). At a longer time, that is, ~2.3 $\mu$s after the pulse when the 420-nm absorption was almost quenched (Figure 2A, curve d), a shoulder located around 300−350 nm is developed. This shoulder then practically disappeared within ca. 30 $\mu$s after the pulse (Figure 2A, curve e), leaving the spectrum, which is characterized by a strong absorption band that steadily increases

below 300 nm with $\lambda_{max} < 270$ nm, whose characteristics appear to be compatible with an assignment to the respective peroxyl radicals RCOO•.[55] In principle, such behavior might indicate the existence of two distinct C•-centered radicals. The first species is characterized by an absorption spectrum with two maxima, one located at $\lambda_{max} = 280$ nm and a second located at $\lambda_{max} = 420$ nm and is identified as the α-(alkylthio)alkyl radical $H_3C-•CH-S-CO-CH_3$. The locations of these two maxima are in reasonably good agreement with those obtained from theoretical calculations. (See Table 2S in Supporting Information.) However, a broad absorption band (Figure 2A) shown as a pronounced shoulder within the range of $\lambda \approx 300-350$ nm could be assigned to two C•-centered radicals: $H_2C•-CH_2-S-CO-CH_3$ and $H_3C-CH_2-S-CO-•CH_2$. The formation of these radicals results from the direct H abstraction from the methyl group adjacent to either the carbonyl group or the methylene by •OH radicals (reactions 12 and 13, respectively).

$$•OH + H_3C-CH_2-S-CO-CH_3 \rightarrow H_3C-CH_2-S-CO-•CH_2 + H_2O \quad (12)$$

$$•OH + H_3C-CH_2-S-CO-CH_3 \rightarrow H_2C•-CH_2-S-CO-CH_3 + H_2O \quad (13)$$

They differ, however, by 4−5 kcal mol$^{-1}$ in stabilization energy (see Table 2S in Supporting Information), with the $H_3C-CH_2-S-CO-•CH_2$ radical being more stable than the $H_2C•-CH_2-S-CO-CH_3$ radical.

We note that the spectra exhibit a weak absorption band with $\lambda_{max} = 540$ nm (Figure 2A). This observation might indicate a small contribution of the C−S bond cleavage in the decay of the monomeric sulfur radical cation that leads to the thiyl-type radicals followed by the formation of thiylperoxyl radicals RSOO•.[56−58]

Similar spectral and kinetic characteristics, as compared with those of the oxygenated aqueous solutions containing a low concentration of SETAc ($10^{-3}$ M), were observed for the oxygenated aqueous solutions containing high concentration of SETAc (50 mM).

*Influence of Oxygen: Neutral Region.* Upon pulse radiolysis of oxygenated aqueous solutions, pH 6, containing 5 mM SETAc, the transient absorption spectrum observed 130 ns after the pulse is characterized by a strong transient absorption that steadily increases below 280 nm and a pronounced absorption band with the maximum located at 360 nm (Figure 2B, curve a). With elapsing time, the absorption band with $\lambda_{max} = 420$ nm becomes more and more pronounced (Figure 2B, curves b and c). The 420-nm absorption band is almost totally quenched within 2.3 μs (Figure 2B, curve d), leaving the spectrum that is characterized by a strong absorption band that steadily increases below 300 nm with $\lambda_{max} < 280$ nm (Figure 2B, curve e). By analogy to similar findings in $O_2$-saturated solutions of SETAc at pH 1 (Figure 2A), these observations confirm earlier assignments of absorptions bands located at 300−420 nm to the combined absorption bands of C•-centered radicals $H_3C-CH_2-S-CO-•CH_2$ and $H_2C•-CH_2-S-CO-CH_3$, absorbing in the region of $\lambda = 320 - 380$ nm and of α-(alkylthio)alkyl radicals ($H_3C-•CH-S-CO-CH_3$) with $\lambda_{max} = 280$ and 420 nm. The formation of these radicals results from the direct H-abstraction by •OH radicals via reactions 12, 13, and 7, respectively.

**Reactions of •H Radicals.** Because some experiments were performed in deoxygenated aqueous solutions at pH 1, the contribution of products formed in reactions of •H radicals to the absorption spectra has to be evaluated. The spectrum in an $N_2O$ saturated solution of SETAc ($10^{-3}$ M) at pH 1 was recorded in the presence of 0.5 M *t*-BuOH. From the available rate constants, we calculated that in the presence of 0.5 M *t*-butyl alcohol ca. 95% of the OH radicals but only ∼2% of the H radicals will be scavenged by *t*-BuOH.[59] Because with thioethers •H radicals do not react with sulfur functionality but solely via H-atom abstraction,[28] the resulting spectrum should represent the transients formed via direct abstraction of hydrogens from SETAc. The transient absorption spectrum recorded 4.3 μs after the pulse (Figure not shown) consists of three weak absorption bands with maxima around 270, 340, and 420 nm with $G \times \epsilon = 700$, 200, and 100 M$^{-1}$ cm$^{-1}$, respectively. These absorption bands are indicative of the presence of C-centered radicals in contrast to the SETAc system without *tert*-butyl alcohol, forming with very low chemical radiation yields.

**Oxidation by Sulfate Radical Anion $SO_4•^-$.** The $SO_4•^-$ radical anion is known to react with thioethers through one-electron oxidation, forming the corresponding monomeric sulfur-centered radical cations. Pulse-radiolysis studies were carried out to generate the transient optical absorption spectrum of (SETAc)>S•$^+$ to obtain quantitative spectral data for (SETAc)>S•$^+$ with the same pulse-radiolysis setup used to obtain transient optical absorption spectra formed during the •OH-induced oxidation of SETAc. The reaction of the $SO_4•^-$ radical anion with SETAc was investigated in Ar-saturated aqueous solution, pH 5.5, containing $10^{-3}$ M SETAc, $5 \times 10^{-3}$ M $K_2S_2O_8$, and 0.5 M *t*-BuOH. The formation of the monomeric sulfur radical cations derived from SETAc occurs through the following reaction:

$$SO_4•^- + H_3C-CH_2-S-CO-CH_3 \rightarrow H_3C-CH_2-S•^+-CO-CH_3 + SO_4^{2-} \quad (14)$$

The transient absorption spectra, at times >1 μs, are reminiscent of the spectrum observed as a result of the oxidation of SETAc by hydroxyl radicals (•OH). Because the 420-nm band is characterized by similar decay kinetic parameters, it can be also assigned to the α-(alkylthio)alkyl radical ($H_3C-•CH-S-CO-CH_3$). Moreover, it can be concluded that (SETAc)>S•$^+$ is very unstable and decays mainly via a deprotonation reaction (reaction 8).

**ESR Studies.** The main component of the ESR signal recorded in a γ-irradiated degassed frozen sample of SETAc studied over the temperature range of 77−95 K was an anisotropic singlet with *g* values of $g_1 = 2.023$, $g_2 = 2.011$, and $g_3 = 2.000$. This spectrum was attributed to the monomeric sulfur radical cation (SETAc)>S•$^+$ formed by the direct ionization of a thioether sulfur. Warming the samples of SETAc to 150 K resulted in the appearance of a multicomponent ESR spectrum (Figure 3A, curve a).

This spectrum can be simulated as a multiline component with $g \approx 2.003$ and hyperfine splittings of $a_{\alpha H} = 2.1$ mT and $a_{\beta H} = 2.6$ mT (Figure 3A, curve b); a second spectrum consisted of four lines with hyperfine splitting of $a_H = 1.75$ mT (Figure 3A, curve c). The first spectrum was assigned to the H-abstraction radical ($H_3C-•CH-S-C(=O)-CH_3$) that might result from the deprotonation of the monomeric sulfur radical cation (SETAc)>S•$^+$. The second spectrum could be attributed to the acyl radical $CH_3CO•$ that might be a product of the fragmentation of (SETAc)>S•$^+$.

**Stable Products.** The γ radiolysis of an $N_2O$-saturated aqueous solution at pH 6 containing SETAc at $10^{-3}$ M concentrations leads to the very low radiation chemical yield of acetaldehyde ($G_{acetaldehyde} = 2 \times 10^{-8}$ mol J$^{-1}$).

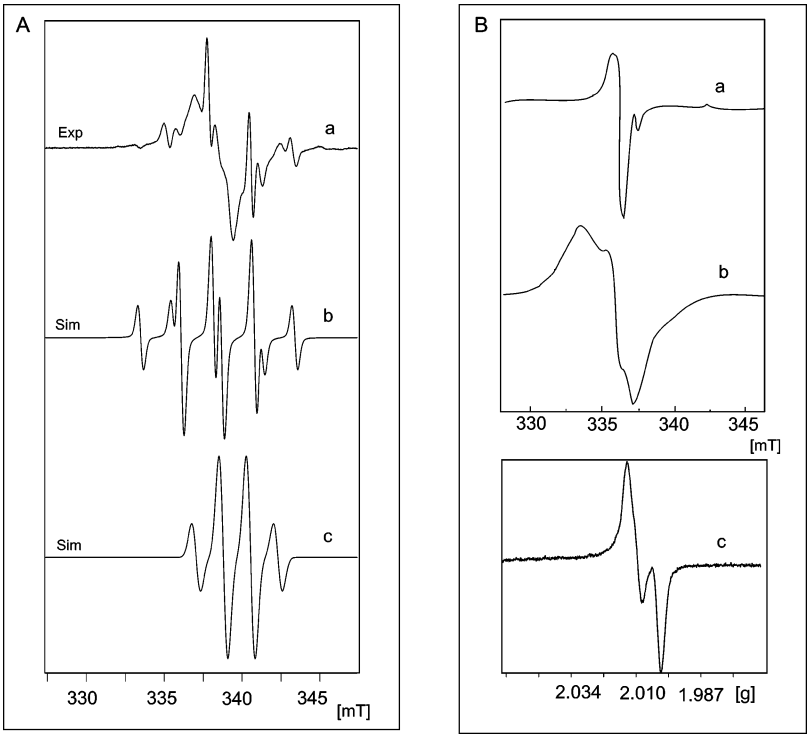


**Figure 3.** (A) ESR spectrum recorded at 150 K and simulated ESR spectra in $\gamma$-irradiated frozen *S*-ethylthioacetate (SETAc) samples: (a) multicomponent experimental spectrum; (b) simulated spectrum of $H_3C-{}^{\bullet}CH-S-C(=O)-CH_3$ radical; and (c) simulated spectrum of $H_3C-CO^{\bullet}$ radical. (B) ESR spectra recorded in $\gamma$ irradiated frozen *S*-ethylthioacetone (SETA) samples: (a) at 95 K; (b) at 110 K (c) at 150 K.

Carbon monoxide was not detected in an $N_2O$-saturated aqueous solution at pH 6 containing SETAc at $10^{-3}$ M concentration.

**Theoretical Studies.** *Hydroxysulfuranyl Radical.* First, we have to determine the possible formation of the hydroxysulfuranyl radical in *S*-ethylthioacetate ($H_3C-CH_2-S^{\bullet}(OH)-CO-CH_3$). Because large discrepancies for the energies appeared between the B3LYP and MP2 methods and from a methodological point of view one has to keep in mind that the B3LYP method very often overestimates the parameters when it is applied to the two-center−three-electron bonds in radicals and radical cations,[44] the MP2/6-31+G* method was used for the calculation of the stabilization energy of $H_3C-CH_2-S^{\bullet}(OH)-CO-CH_3$. This method was successfully applied to dimethyl sulfide.[47,60] Within the MP2 method, no minimum was found in the calculations of the bond formation energy for the $^{\bullet}OH$ adduct in *S*-ethylthioacetate. Note that this result is in agreement with the experimental observations (vide supra) and shows that the strong electron-withdrawing acetyl group that is linked directly to the sulfur atom does not favor the formation of the $^{\bullet}OH$ adduct.

*Monomeric Sulfur Radical Cation ($R_2S^{+\bullet}$).* Because the electron is localized in the monomeric sulfur radical cation, both the MP2 and the B3LYP methods were applied and gave similar results.[60] The respective bond-formation energies are calculated considering only energetic factors and assuming that the following two processes lead to the formation of $H_3C-CH_2-S^{+\bullet}-CO-CH_3$ (reactions 15 and 16):

$$H_3C-CH_2-S-CO-CH_3 + {}^{\bullet}OH \rightarrow H_3C-CH_2-S^{+\bullet}-CO-CH_3 + OH^- \quad (15)$$

$$H_3C-CH_2-S-CO-CH_3 + {}^{\bullet}OH + H_3O^+ \rightarrow H_3C-CH_2-S^{+\bullet}-CO-CH_3 + 2H_2O \quad (16)$$

The respective bond formation energies $\Delta E'$ and $\Delta E''$ are defined as follows:

$$\Delta E' = E(H_3C-CH_2-S^{+\bullet}-CO-CH_3) + E(OH^-) - E(H_3C-CH_2-S-CO-CH_3) - E({}^{\bullet}OH)$$

and

$$\Delta E'' = E(H_3C-CH_2-S^{+\bullet}-CO-CH_3) + 2E(H_2O) - E(H_3C-CH_2-S-CO-CH_3) - E({}^{\bullet}OH) - E(H_3O^+)$$

Their values are listed in Supporting Information, Table 2S. The unfavorable formation of the monomeric sulfur radical cation is clearly evident from these data.

The calculations of optical absorption peaks together with dipole oscillator strenghts that were carried out with the density functional B3PW91 with the extended basis set, cc-pVTZ (see Supporting Information, Table 2S), show that the locations of the calculated absorption maximum are shifted to the UV compared to those of the experiment. This is caused by the limits of the calculation methods (vide supra). Nevertheless, it seems that the calculated 322-nm absorption for the monomeric sulfur radical cation $H_3C-CH_2-S^{+\bullet}-CO-CH_3$ is reasonably well related to the experimentally observed absorption maximum for this species located in the 340−360 nm region.

*Dimeric Sulfur Radical Cation ($R_2S\therefore SR_2)^+$.* Dimeric sulfur radical cations are formed via dimerization of the monomeric sulfur radical cation ($R_2S^{+\bullet}$) with the parent molecule ($R_2S$). Dimeric sulfur radical cations contain two-center−three-electron (2c, 3e) sulfur−sulfur bonds; therefore, calculations were performed using the MP2/6-31G+G(d) method. Because of the size of the ethyl substituent, calculations of the bond formation energy were performed for S-methylthioacetone. The bond formation energy ($\Delta E'$) of the

dimeric sulfur radical cation of methylthioacetate is defined as follows:

$$\Delta E' = E[(H_3C)(CH_3{-}CO){>}S\therefore S{<}(H_3C{-}CO)(CH_3)]^+ - E(H_3C{-}S^{+\bullet}{-}CO{-}CH_3) - E(H_3C{-}S{-}CO{-}CH_3)$$

It is listed in Table 2S (Supporting Information). It is evident that the dimeric sulfur radical cation is stable as most of the 2c−3e bonded [>S∴S<].[61] Generally, three-electron-bonded dimeric sulfur radical cations are experimentally easily observable,[5] so the failure in detecting dimeric sulfur radical cations of SETAc (vide supra) is due to the low stability of the precursor, that is, the sulfur monomeric radical cation (SETAc)>S$^{\bullet+}$ and/or the low efficiacy of reaction 11 (vide supra).

*C*$^\bullet$*-Centered Radicals.* The homolytic abstraction of hydrogen from either the methylene group or one of two methyl groups (one is located in the vicinity of the carbonyl group, the second one is in the vicinity of the methylene group) was considered for SETAc. For these radicals, because the electron is localized, both the MP2 and B3LYP methods were used and gave very similar results.[60] The calculations of bond-formation energies performed using the B3LYP method show that these three C$^\bullet$-centered radicals are stable. (See Table 2S in Supporting Information). The bond formation energies of the C$^\bullet$-centered radicals are calculated considering only energetic factors and assuming their formation via direct hydrogen abstraction from the parent molecule by hydroxyl radicals:

$$\Delta E' = (E(R_1{-}S{-}R_2(-H)C^\bullet) + E(H_2O) - E(R_1{-}S{-}R_2) - E(^\bullet OH)$$

An additional reaction pathway involving the monomeric sulfur radical cation ($H_3C{-}CH_2{-}S^{\bullet+}{-}C(=O){-}CH_3$) for the formation of the C$^\bullet$-centered radical ($H_3C{-}{}^\bullet CH{-}S{-}C(=O){-}CH_3$) was considered

$$\Delta E'' = E[R_1{-}S{-}R_2(-H)C^\bullet] + E(H_3O^+) - E(R_1{-}S^{\bullet+}{-}R_2) - E(H_2O)$$

As can be seen from Table 2S (Supporting Information), the formation of two C$^\bullet$-centered radicals, $H_3C{-}CH_2{-}S{-}C(=O){-}{}^\bullet CH_2$ and $H_3C{-}{}^\bullet CH{-}S{-}C(=O){-}CH_3$, via the abstraction of hydrogen by $^\bullet$OH radicals seems to be the most favorable. The enhanced stability of these radicals is rationalized by the location of stabilizing carbonyl and thioether groups with respect to the radical site, respectively.

The calculations of optical absorption peaks were carried out with two methods: B3LYP/6-31G* and the density functional B3PW91 with the extended basis set, cc-pVTZ, which give similar results. The peaks of optical absorptions, together with the dipole oscillator strengths, are presented in Table 2S (Supporting Information). It is evident that the locations of calculated absorption maxima are shifted to the UV as compared with those of the experiment. This is again caused by the limits of calculation methods. (See Experimental Section.) Nevertheless, the calculated 384-nm absorption for the $H_3C{-}{}^\bullet CH{-}S{-}C(=O){-}CH_3$ radical is reasonably well related to the experimentally observed absorption maximum for this radical at $\lambda =$ 420 nm.

***S*-Ethylthioacetone (SETA).** With respect to sulfur, SETA contains a $\beta$-positioned acetyl group. The reaction of $^\bullet$OH radicals with SETA was investigated in $N_2O$-saturated solutions over the concentration range of $2 \times 10^{-4}$−$5 \times 10^{-2}$ M and the pH range of 1−6.

**Mechanistic Studies with the Hydroxyl Radical.** *Influence of pH.* Depending on the pH, pulse irradiation leads to different transient optical spectra. The absorption spectrum obtained 330 ns after pulse irradiation of an $N_2O$-saturated aqueous solution, pH 1, containing $10^{-3}$ M SETA is displayed in Figure 4A (curve a).

It is characterized by two distinctive absorption bands with maxima located at $\lambda_{max} = 290$ and 380 nm and a pronounced shoulder with a maximum around 500 nm. They are formed with radiation chemical yields of $G \times \epsilon_{290} = 16\,000$ M$^{-1}$ cm$^{-1}$, $G \times \epsilon_{380} = 7300$ M$^{-1}$ cm$^{-1}$, and $G \times \epsilon_{500} = 2200$ M$^{-1}$ cm$^{-1}$, respectively. The transient absorption around 500 nm practically dissappeared within 30 $\mu$s after the pulse (Figure 4A, inset), leaving two UV bands with $\lambda_{max} = 290$ and 380 nm (Figure 4A, curves b,−d). It may be anticipated, and is supported by experimental findings (vide infra), that the spectrum represented by a pronounced shoulder around 500 nm could be assigned to the intermolecular dimeric three-electron-bonded sulfur radical cation (SETA)(S∴S)$^+$. A distinct absorption band with $\lambda_{max} =$ 290 nm indicates the presence of α-(alkylthio)-alkyl radicals, which can be formed either via direct hydrogen abstraction from the adjacent methylene groups (reaction 17a and b)

$$^\bullet OH + H_3C{-}CH_2{-}S{-}CH_2{-}CO{-}CH_3 \rightarrow H_3C{-}CH_2{-}S{-}{}^\bullet CH{-}CO{-}CH_3 + H_2O \quad (17a)$$

$$^\bullet OH + H_3C{-}CH_2{-}S{-}CH_2{-}CO{-}CH_3 \rightarrow H_3C{-}{}^\bullet CH{-}S{-}CH_2{-}CO{-}CH_3 + H_2O \quad (17b)$$

or via deprotonation of the monomeric sulfur radical cation (SETA)>S$^{\bullet+}$ in reaction 18a and 18b:

$$H_3C{-}CH_2{-}S^{\bullet+}{-}CH_2{-}CO{-}CH_3 \rightarrow H_3C{-}CH_2{-}S{-}{}^\bullet CH{-}CO{-}CH_3 + H^+ \quad (18a)$$

$$H_3C{-}CH_2{-}S^{\bullet+}{-}CH_2{-}CO{-}CH_3 \rightarrow H_3C{-}{}^\bullet CH{-}S{-}CH_2{-}CO{-}CH_3 + H^+ \quad (18b)$$

which are analogous to reaction 8.

At this point in the exposition, we are not able to assign definitively the 380-nm absorption band to the particular intermediate. In principle, the shape of the absorption band and the location of the absorption maximum might indicate the presence of the intramolecularly ($^\bullet$S−O)-bonded species involving the oxygen located in the carbonyl group. However, the formation of the ($^\bullet$S−O)-bonded species would require a sterically unfavorable four-membered ring structure. Therefore, that species can be excluded on the basis of previous unsuccessful attempts to observe such structures. An assignment of the 380-nm will be discussed later (vide infra).

The transient absorption spectrum observed 330 ns after the pulse irradiation of an $N_2O$-saturated solution of $10^{-3}$ M SETA at pH 6 (Figure 4B, curve a) exhibits an intense band with a maximum at $\lambda_{max} = 340$ nm, formed with a radiation chemical yield of $G \times \epsilon_{340} = 17\,000$ M$^{-1}$ cm$^{-1}$. Its intensity is considerably reduced in the presence of 0.5 M *tert*-butyl alcohol. Thus, the 340-nm band is caused by the reaction of $^\bullet$OH radicals with SETA and furthermore, on the basis of previous

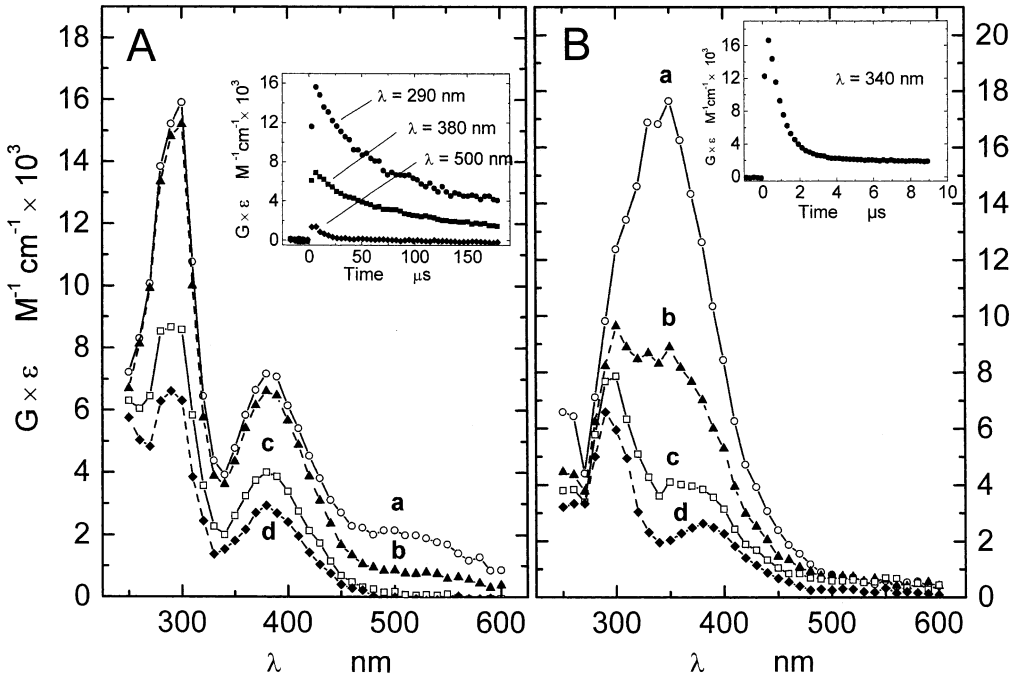


**Figure 4.** Transient absorption spectra observed in $N_2O$-saturated aqueous solution containing $10^{-3}$ M *S*-ethylthioacetone (SETA): (A) (○) 330 ns, (▲) 10 $\mu$s, (□) 50 $\mu$s, and (◆) 90 pulse irradiation at pH 1. Inset: kinetic traces of decays of the 290-, 380-, and 500-nm absorbances. (B) (○) 330 ns, (▲)1 $\mu$s, (□), 2 $\mu$s, and (◆) 10 $\mu$s after pulse irradiation at pH 6. Inset: kinetic trace for a decay of the 340-nm absorbance.

findings,[14−16,62] is assigned to the hydroxysulfuranyl radicals that are formed according to reaction 19:

$$^{\bullet}OH + H_3C-CH_2-S-CH_2-CO-CH_3 \rightarrow H_3C-CH_2-S^{\bullet}(OH)-CH_2-CO-CH_3 \quad (19)$$

The division of $G \times \epsilon_{340}$, by the maximum radiation chemical yield of $G(^{\bullet}OH) = 5.6$ yields an apparent extinction coefficient of $\epsilon_{340} = 3050\ M^{-1}\ cm^{-1}$. The latter value of the apparent extinction coefficient clearly indicates that the hydroxysulfuranyl radicals are formed with almost 100% of the available $^{\bullet}OH$ radicals because the calculated $\epsilon_{340}$ fits very well into the range of 3000−4000 $M^{-1}\ cm^{-1}$ that is typical for such adducts.[15,16]

The 340-nm absorption band subsequently decays within a 3-$\mu$s time domain (inset in Figure 4B), leaving the transient spectrum with two distinctive absorption bands with maxima located at $\lambda_{max} = 290$ and 380 nm (Figure **4**B, curve d). The resulting spectrum is identical with regard to the position of the absorption maxima to that of the spectrum recorded in $N_2O$-saturated solutions at pH 1 after the decay of the 500-nm band (Figure 4A, curves c and d). It is noteworthy that no absorption in the region of 500 nm indicative of the formation of the intermolecular dimeric three-electron-bonded sulfur radical cation $(SETA)(S\therefore S)^+$ was observed after pulse irradiation of solutions containing SETA at pH 6 (Figure 4B).

*Influence of Concentration.* Because low pH and high concentrations of thioethers facilitate the formation of intermolecular dimeric sulfur-centered radical cations, the behavior of the 500-nm absorption band can be probed at higher concentrations of SETA. To confirm whether an assignment of 500-nm absorption band to the intermolecular dimeric three-electron-bonded sulfur radical cation $(SETA)(S\therefore S)^+$ is correct, we performed pulse radiolysis experiments in aqueous solutions of pH 1 with various concentrations, $10^{-3}$ to $5 \times 10^{-2}$ M, of SETA. It can be seen in Figure 5A (inset) that the transient spectra recorded 330 ns after the electron pulse change substantially with increasing concentration of SETA.

The intensity of the 500-nm absorption band expressed as $G \times \epsilon_{500}$ increases with the concentration of SETA from $G \times \epsilon_{500} = 2000\ M^{-1}\ cm^{-1}$ (for $10^{-3}$ M) (Figure 5A, curve a in inset) up to $G \times \epsilon_{500} = 17\,000\ M^{-1}\ cm^{-1}$ (for $5 \times 10^{-2}$ M) (Figure 5A, curve e in inset). On the basis of the formula given by Schuler et al.,[54] which relates the *G* value of solute radicals generated by $^{\bullet}OH$ radicals to the product of the rate constant for the reaction of $^{\bullet}OH$ radicals with the solute and the solute concentration, one can calculate that the *G* value of $^{\bullet}OH$ radicals available for the reaction with SETA and also that the *G* value of the immediate oxidation product $(SETA)>S^{\bullet+}$ can be increased by only ∼15−20% with increasing SETA concentration from $10^{-3}$ M to $5 \times 10^{-2}$ M. Therefore, one can conclude that an intermediate whose absorption spectrum is maximized at 500 nm is due to the dimeric sulfur-centered radical cation $(SETA)(S\therefore S)^+$.

It can be seen in Figure 5A that the transient spectra recorded at pH 1 for the very high concentration (25 mM) of SETA change substantially with elapsing time. The transient spectrum recorded 130 ns after the electron pulse is dominated by an absorption band with $\lambda_{max} = 500$ nm formed with a radiation chemical yield of $G \times \epsilon_{500} = 15\,000\ M^{-1}\ cm^{-1}$ and a pronounced shoulder around 350−400 nm (Figure 5A, curve a). The 500-nm absorption that is assigned to the dimeric sulfur-centered radical cation $(SETA)(S\therefore S)^+$ decreases significantly over the single-microsecond time domain after the pulse, leaving two UV bands, one with $\lambda_{max} \approx 390-400$ nm (Figure 5A, curves c and d) and the second one with its maximum below 320 nm. These two spectra resemble the spectra recorded in $N_2O$-saturated solutions at the lower concentration ($10^{-3}$ M) of SETA, 330 ns after the electron pulse at pH 1 (Figure 4A, curve a) and 10 $\mu$s after the electron pulse at pH 6 (Figure 4B, curve d).

It appears very surprising that the transient absorption spectra recorded in an $N_2O$-saturated solution at pH 6 for the very high concentration (25 mM) of SETA before and after the completion of the decay of the hydroxysulfuranyl radicals (Figure 5B, curves a and c) are not reminiscent at all of the spectrum obtained by

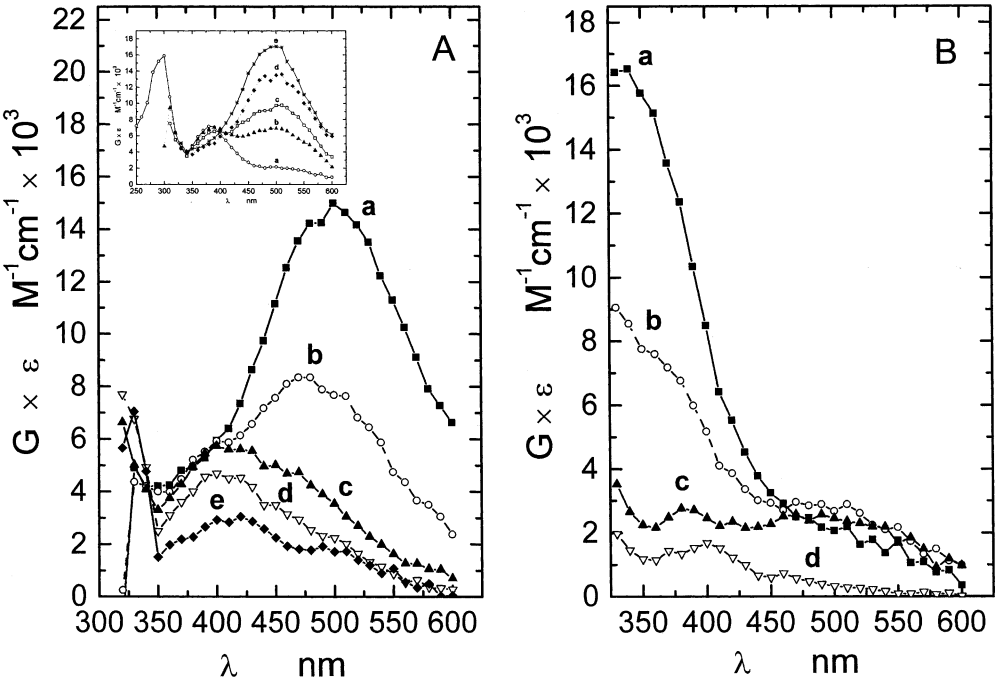


**Figure 5.** (A) Transient absorption spectra observed in $N_2O$-saturated aqueous solution at pH 1 containing $2.5 \times 10^{-2}$ M *S*-ethylthioacetone (SETA): (■) 130 ns, (○) 2 $\mu$s, (▲) 5 $\mu$s, (▽) 18 $\mu$s, and (◆) 74.4 $\mu$s after pulse irradiation. Inset: transient absorption spectra observed 330 ns after pulse irradiation in $N_2O$-saturated aqueous solution at pH 1 containing (○)$10^{-3}$ M, (▲) $5 \times 10^{-3}$ M, (□)$10^{-2}$ M, (◆) $2.5 \times 10^{-2}$ M, and (*) $5 \times 10^{-2}$ M *S*-ethylthioacetone (SETA). (B) Transient absorption spectra observed in $N_2O$-saturated aqueous solution at pH 6 containing $2.5 \times 10^{-2}$ M S-ethylthioacetone (SETA): (■) 380 ns, (○) 830 ns, (▲) 2 $\mu$s, and (▽) 18 $\mu$s after pulse irradiation.

us at pH 1 for the same concentration (25 mM) of SETA (Figure 5A, curve d in inset). The spectrum recorded 380 ns after the electron pulse exhibits an intense absorption band with $\lambda_{max} =$ 340 nm with the radiation chemical yield of $G \times \epsilon_{340} = 16\,500$ $M^{-1}$ $cm^{-1}$ and a weak absorption band with $\lambda_{max} = 500$ nm with the radiation chemical yield of $G \times \epsilon_{500} = 2000$ $M^{-1}cm^{-1}$ (Figure 5B, curve a). Two intermediates could be identified from the composite spectrum. The transient at 340 nm represents the hydroxysulfuranyl radical (SETA)$>$S$^{\bullet}$-OH, and that at 500 nm is assigned to the dimeric sulfur-centered radical cation (SETA)-$(S\therefore S)^+$. The spectrum obtained after the decay of the hydroxysulfuranyl radical exhibits a very broad absorption band in the region from 320 to 600 nm, with two maxima located at $\lambda_{max}$ = 380 and 500 nm with the respective $G \times \epsilon = 2900$ and 2800 $M^{-1}$ $cm^{-1}$ (Figure 5B, curve c). This reveals another interesting feature that indicates that hydroxysulfuranyl radicals (SETA)$>$S$^{\bullet}$-OH are not efficiently converted into (SETA)$(S\therefore S)^+$ because they would rather convert into the 380-nm species. However, such a rationale would imply the existence of another mechanism leading to the decomposition of (SETA)$>$S$^{\bullet}$-OH besides spontaneous unimolecular hydroxide elimination leading to the formation of monomeric sulfur-centered radical cation (SETA)$>$S$^{\bullet+}$ or, subsequently, its dimeric form (SETA)$(S\therefore S)^+$.

*Influence of Oxygen.* Upon pulse radiolysis of oxygenated aqueous solutions, pH 1, containing $10^{-3}$ M SETA, the transient absorption spectrum observed 330 ns after the pulse is characterized by two distinctive absorption bands with maxima located at $\lambda_{max} = 290$ and 380 nm and a pronounced shoulder with a maximum around 500 nm (Figure 6, curve a).

They are formed with radiation chemical yields of $G \times \epsilon_{290}$ $= 9200$ $M^{-1}cm^{-1}$, $G \times \epsilon_{380} = 4200$ $M^{-1}cm^{-1}$, and $G \times \epsilon_{500} =$ 1700 $M^{-1}cm^{-1}$, respectively. By analogy to similar findings in $N_2O$-saturated solutions (Figure 4A, curve a), the 290- and 500-nm absorption bands indicate the presence of α-(alkylthio)alkyl radicals and (SETA)$(S\therefore S)^+$, respectively. The intensity of the absorption bands and the decay kinetics measured at $\lambda_{max} =$ 290 and 380 nm are affected in the same way by the presence of oxygen, suggesting that both absorption bands can be assigned to the same radical, that is, the α-(alkylthio)alkyl radical (Figure 6, left inset). In the presence of oxygen, this C$^{\bullet}$-centered radical converts into its respective peroxyl radical (Figure 6, curve d). Theoretical caluclations show (vide infra) that the C$^{\bullet}$-centered radical resulting from the H abstraction from the carbon of the methylene group located between the sulfur atom and the acetyl group (reaction 18a) is the most stable C$^{\bullet}$-centered radical derived from SETA. Its respective formation energy is ∼13 kcal $mol^{-1}$ lower than the formation energies of two other radicals derived from SETA, that is, $H_3C-{}^{\bullet}CH-S-CH_2-CO-CH_3$ and $H_3C-CH_2-S-CH_2-CO-{}^{\bullet}CH_2$. (See Table 3S in Supporting Information.) Therefore, it is reasonable to assign the 380-nm absorption band exclusively to the $H_3C-CH_2-S-{}^{\bullet}CH-CO-CH_3$ radical.

**Reactions with $^{\bullet}$H Radicals.** The transient absorption spectrum recorded 4.3 $\mu$s after pulse irradiation of the $N_2O$-saturated solution, pH 1, containing $10^{-3}$ M SETA and 0.5 M *t*-BuOH consists of three weak absorption bands with maxima around 270, 320, and 380 nm with $G \times \epsilon = 500$, 400, and 200 $M^{-1}$ $cm^{-1}$, respectively. These absorption bands are indicative of the presence of C-centered radicals in contrast to the SETA system without *t*-BuOH, forming with very low radiation chemical yields. In particular, the absorption band at 380 nm can be attributed to the α-(alkylthio)alkyl radical $H_3C-CH_2-S-{}^{\bullet}CH-CO-CH_3$.

**Oxidation by Sulfate Radical Anion $SO_4^{\bullet-}$.** A transient spectrum with two distinctive absorption bands with maxima located at $\lambda_{max} = 290$ and 380 nm and $G \times \epsilon_{290} = 2750$ $M^{-1}cm^{-1}$and $G \times \epsilon_{380} = 1250$ $M^{-1}cm^{-1}$ was seen 1 $\mu$s after the radiolytic pulsing of an aqueous Ar-saturated solution containing 1 mM SETA, 5 mM $K_2S_2O_8$, and 0.5 M *t*-BuOH at pH 5.5 (Figure 6, curve a in right inset).

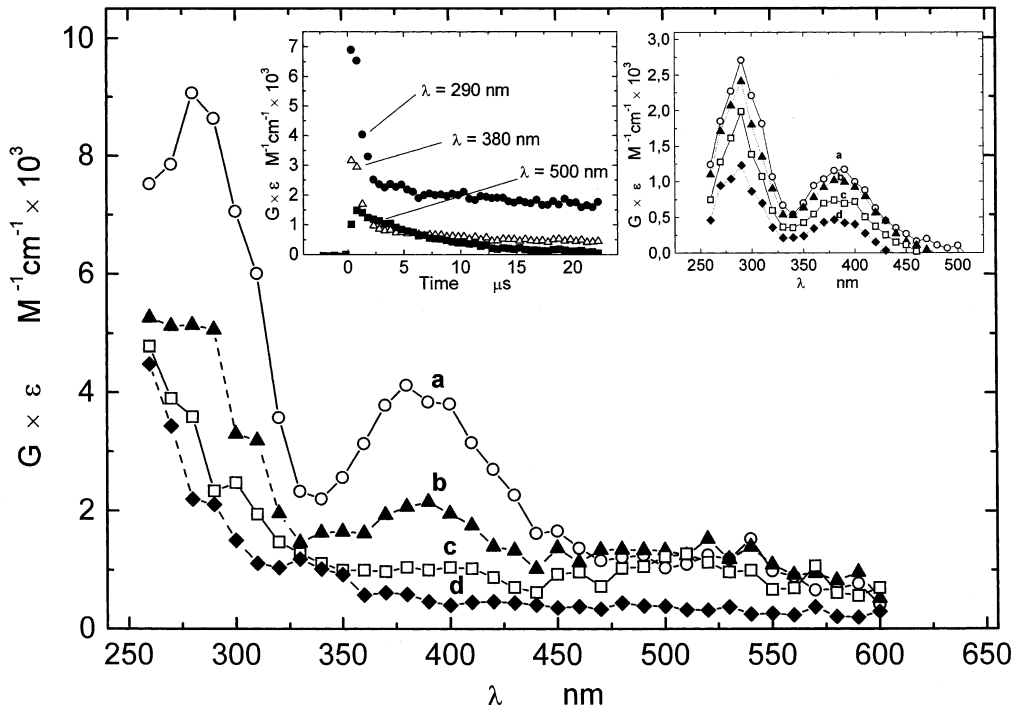


**Figure 6.** Transient absorption spectra observed in $O_2$-saturated aqueous solution at pH 1 containing $10^{-3}$ M *S*-ethylthioacetone (SETA): (○) 330 ns, (▲) 1 $\mu$s, (□) 2 $\mu$s, and (◆) 10 $\mu$s after pulse irradiation. Insets: (left) kinetic traces of decays of the 290-, 380-, and 500-nm absorbances; (right) transient absorption spectra observed in Ar-saturated aqueous solution at pH 5.5 containing $10^{-3}$ M *S*-ethylthioacetone (SETA), $5 \times 10^{-3}$ M $K_2S_2O_8$, and 0.5 M *tert*-butyl alcohol (○) 1 $\mu$s, (▲) 20 $\mu$s, (□) 50 $\mu$s, and (◆) 100 $\mu$s after pulse irradiation.

The formation of the monomeric sulfur radical cations derived from SETA occurs through reaction 20:

$$SO_4^{\bullet-} + H_3C-CH_2-S-CH_2-CO-CH_3 \rightarrow H_3C-CH_2-S^{\bullet+}-CH_2-CO-CH_3 + SO_4^{2-} \quad (20)$$

Because the transient absorption spectra, at times longer than 1 $\mu$s (Figure 6, curves b−d in right inset), are reminiscent of the spectra observed as a result of the oxidation of SETA at pH 1 and low concencentration (1 mM) by hydroxyl radicals ($^{\bullet}$OH) and are characterized by similar decay kinetic parameters, they can also be assigned to the α-(alkylthio)alkyl radical $H_3C-CH_2-S-{}^{\bullet}CH-CO-CH_3$. Therefore, it can be concluded that the sulfur-centered radical cation $H_3C-CH_2-S^{+\bullet}-CH_2-CO-CH_3$ is very unstable and decays on the submicrosecond time range, forming 380-nm species.

**ESR Studies.** The main component of the ESR signal recorded in a $\gamma$-irradiated degassed frozen sample of SETA studied over the temperature range of 77−95 K was an anisotropic singlet with $g$ values of $g_1 = 2.023$, $g_2 = 2.011$, and $g_3 = 2.000$ (Figure 3B, curve a). This spectrum was attributed to the monomeric sulfur radical cation (SETA)>$S^{\bullet+}$ formed by the direct ionization of a thioether sulfur. Warming the samples of SETA to 100−110 K resulted in the appearance of a broad singlet ESR signal with $g_{av} = 2.01$ (Figure 3B, curve b). The singlet can be attributed to the dimeric sulfur-centered radical cation (SETA)$(S\therefore S)^+$. As the temperature was increased to 150 K, the ESR spectrum represents a doublet with $g_{av} = 2.0045$ and a hyperfine splitting of $a_H = 1.4$ mT (Figure 3B, curve c). This spectrum was assigned to the carbon-centered radical ($H_3C-CH_2-S-{}^{\bullet}CH-CO-CH_3$) that might result from the deprotonation of the monomeric radical cation (SETA)>$S^{\bullet+}$.

**Theoretical Studies.** *Hydroxysulfuranyl Radical.* Calculations were performed for the *S*-ethylthioacetone ($H_3C-CO-CH_2-S-CH_2-CH_3$) molecule to determine the influence of the acetyl group on the stability of the hydroxysulfuranyl radical that is separated from the sulfur atom by a methylene group. The results obtained for the bond-formation energies are summarized in Table 3S. (See Supporting Information.) When considering the OH adduct of SETA in vacuo, it has to be stressed that the OH adduct has the character of a stable intermediate. The formation energy of a sulfur−oxygen bond is smaller than that of a covalent bond; however, it is comparable to the formation energy of a sulfur−oxygen bond that was calculated for the the OH adduct in dimethyl sulfide (DMS).[47,60] The electron-releasing methyl groups adjacent on both sides to the sulfur atom in DMS compared to the electron-releasing alkyl groups (one of them adjacent to the electron-withdrawing carbonyl group) in SETA might affect the electron density on the sulfur atom in slightly different way. As we have recently pointed out for DMS−OH,[63] the spin density is quasi equally shared between both S and O atoms, which characterizes the (2c, 3e) bonds. This is reflected in different bond-formation energies of the OH adducts: −8.6 kcal mol$^{-1}$ in dimethyl sulfide[47,60,63,64] and −5.6 kcal mol$^{-1}$ in *S*-ethylthioacetone.[60] However, when electronic factors are favorable, these bond-formation energies dramatically decrease in aqueous solutions to −1.8 kcal mol$^{-1}$ in dimethyl sulfide[60] and +0.96 kcal mol$^{-1}$ in *S*-ethylthioacetone. (See Table 3S in Supporting Information.) Furthermore, B3LYP calculations were carried out, though we are aware that the method is not the most appropriate and very often overestimates the bond-formation energy. In light of the experimental observation of the OH adduct, the calculated value of −7.9 kcal mol$^{-1}$ (compared to −3.7 kcal mol$^{-1}$ obtained by McKee with B3LYP for DMS)[64] for the bond formation energy might suggest that the real value is located between the two calculated values, +0.96 and −7.9 kcal mol$^{-1}$.

The calculated absorption peak of $\lambda = 318$ nm provides additional support for the proposed assignment of the transient spectrum with $\lambda_{max} = 340$ nm to the hydroxysulfuranyl radical.

*Monomeric Sulfur Radical Cation ($R_2S^{+\bullet}$).* The respective bond-formation energies ($\Delta E'$ and $\Delta E''$), defined in a similar way as those for *S*-ethylthioacetate, are summarized in Table 3S. (See Supporting Information). The favorable formation of the monomeric sulfur radical cation is clearly evident when hydronium ions are involved in the reaction.

*Dimeric Radical Cations ($R_2S\therefore SR_2)^+$.* Calculations of the bond-formation energy of the dimeric sulfur radical cations were not performed mainly because of the size of the transient entity. The similarity of other calculated parameters of transients (OH adducts and sulfur monomeric radical cations) in SETA and DMS[60] justifies the extrapolation of the bond-formation energy of the dimeric sulfur radical cation from that obtained for DMS. The value obtained for the dimeric radical cation of DMS is taken as a good estimate of the bond-formation energy of the dimeric sulfur radical cation of SETA. (See Table 3S in Supporting Information.)

*C$^\bullet$-Centered Radicals.* For SETA, we considered the homolytic abstraction of hydrogen either from the two methylene groups adjacent on both sides to the sulfur atom or from the two methyl groups (one located in the vicinity of the carbonyl group, and the second one located in the vicinity of the methylene group). For these radicals, because the electron is localized, the MP2 and B3LYP methods were used and gave very similar results. The respective bond-formation energies ($\Delta E'$ and $\Delta E''$), defined in a similar way as those for *S*-ethylthioacetate, are summarized in Table 3S. (See Supporting Information.) An additional reaction pathway involving the monomeric sulfur radical cation ($H_3C-CH_2-S^{\bullet+}-CH_2-C(=O)-CH_3$) was considered for the formation of two C$^\bullet$-centered radicals, $H_3C-CH_2-S-{}^\bullet CH-C(=O)-CH_3$ and $H_3C-{}^\bullet CH-S-CH_2-C(=O)-CH_3$. The calculations performed show that these four C$^\bullet$-centered radicals are stable. In particular, the formation of one of the C$^\bullet$-centered radicals, $H_3C-CH_2-S-{}^\bullet CH-C(=O)-CH_3$, via hydrogen abstraction by $^\bullet$OH radicals, seems to be very favorable. Its respective formation energy is lower by $\sim$13 kcal mol$^{-1}$ than the formation energies of $H_3C-{}^\bullet CH-S-CH_2-C(=O)-CH_3$ and $H_3C-CH_2-S-CH_2-C(=O)-{}^\bullet CH_2$ radicals and lower by $\sim$19 kcal mol$^{-1}$ than the formation energy for $H_2C^\bullet-CH_2-S-CH_2-C(=O)-CH_3$.

The calculated absorption peak of $\lambda = 322$ nm provides support for the proposed assignment of the transient spectrum with $\lambda_{max} = 380$ nm to the $H_3C-CH_2-S-{}^\bullet CH-C(=O)-CH_3$ radical.

## Discussion

**Assignments of 420- and 350-nm Absorption Bands in SETAc.** Because the radiation chemical yields, expressed as $G \times \epsilon_{420}$, increase by only $\sim$10% with increasing SETAc concentration, support might be provided for a tentative assignment of the 420-nm absorption band to the monomeric sulfur radical cation (SETAc)$>S^{\bullet+}$. This assignment is in agreement with our earlier studies on *N*,*S*-diacetyl-L-cysteine ethyl ester (SNACET).[34] However, the following key features point to the α-(alkylthio)alkyl radical ($H_3C-{}^\bullet CH-S-CO-CH_3$) as the species responsible for the 420-nm absorption: (i) the decay rate of the 420-nm absorption is more than 1 order of magnitude smaller than the reported value for SNACET; (ii) the decay rate of the 420-nm absorption is not affected by SETAc concentration; however, it is affected by oxygen concentration; (iii) the intensity of the 420-nm absorption (expressed as $G \times \epsilon_{420}$) is about 2.5-fold lower in comparison to that of SNACET solutions measured under similar experimental conditions (concentration, pH); and (iv) a different pattern of the pH dependence for $G \times \epsilon_{420}$ manifested as a shift of the inflection point (from 2.1 to 3.3) and a higher normalized $G \times \epsilon_{420}$ plateau level (40 vs 5%) was measured above the inflection point in comparison to that of SNACET. Accordingly, we conclude that the decay observed at $\lambda = 420$ nm can be rationalized by the decay of α-(alkylthio)-alkyl radicals ($H_3C-{}^\bullet CH-S-CO-CH_3$) via dimerization and/or disproportionation.

The assignment of the short-lived absorption band located within the 340−360-nm region from the sulfur monomeric radical cation SETAc($>S^{+\bullet}$) needs justification. The reaction of $^\bullet$OH radicals with SETAc should initially yield the hydroxysulfuranyl radicals, which at low pH decompose into monomeric sulfur radical cations SETAc($>S^{+\bullet}$) via the proton-assisted elimination of water. The fast formation in very acidic solutions (pH 1) of the 350-nm absorption as a primary absorption band and no oxygen influence on its decay seem to corroborate this assignment. Moreover, the decay of the 350-nm absorption is accompanied by the simultaneous formation of the 420-nm absorption, and neither process affected by the SETAc concentration. Because SETAc($>S^{+\bullet}$) might either decompose via irreversible deprotonation or associate intermolecularly with a second SETAc molecule, the decay of absorption observed at 350 nm and the formation of absorption at 420 nm can be reasonably rationalized as a transformation of the SETAc($>S^{+\bullet}$) into the α-(alkylthio)alkyl radical ($H_3C-{}^\bullet CH-S-CO-CH_3$) via the deprotonation process.

**$^\bullet$OH-Induced Oxidation Mechanism of SETAc.** The following observations have to be considered in the elaboration of the mechanism of the $^\bullet$OH-induced oxidation of SETAc: (i) the oxidation leads predominantly to the α-(alkylthio)alkyl radical $H_3C-{}^\bullet CH-S-CO-CH_3$ with some contribution of the C-centered radicals $H_3C-CH-S-CO-{}^\bullet CH_2$ at high and low proton concentrations; (ii) hydroxysulfuranyl radicals ($H_3C-CH_2-{}^\bullet S(OH)-CO-CH_3$) are very short-lived at low proton concentration, if they are formed at all; (iii) low yields of thiylperoxyl radicals are observed in the presence of oxygen; and (iv) the oxidation results in small yields of acetaldehyde.

The first step in the reaction of hydroxyl radicals with SETAc is an addition to the sulfur atom (Scheme 1, reaction 1.1)and an abstraction of hydrogen atoms from the methylene group adjacent to the thioether group (Scheme 1, reaction 1.2) and from the methyl group adjacent to the carbonyl group (Scheme 1, reaction 1.3), leading to the formation of hydroxysulfuranyl-type radicals (**1.1a**), α-(alkylthio)alkyl radicals (**1.2**), and alkyl-substitued radicals (**1.3**), respectively. At high proton concentration, the initially formed **1.1a** radicals undergo a very fast proton-catalyzed elimination of hydroxide ions (Scheme 1, reaction 1.4). This reaction channel provides the basis for the observation of the monomeric sulfur radical cations (**1.4**) characterized by an optical absorption with $\lambda_{max}$ located in the 340−360-nm region. In principle, **1.4** radical cations are expected to be in equilibrium with the intermolecularly three-electron-bonded SETAc$(S\therefore S)^+$. The lack of a characteristic absorption band that could be assigned to such species, consistent with the fact that the decay kinetics of **1.4** is not affected by SETAc concentration indicates that the existence of such an equilibrium is negligible. The second anticipated reaction channel of **1.4** is irreversible deprotonation (Scheme 1, reaction 1.5) that occurs with the rate constant in the range of $4.9 \times 10^6$ s$^{-1}$ and leads to the formation of **1.2** radicals, characterized by an optical absorption spectrum with $\lambda_{max} =$ 420 nm. It is also noteworthy that the observation of peroxyl radicals RSOO$^\bullet$ in oxygenated SETAc acidic solutions suggests that the fragmentation of **1.4** involving C−S bond cleavage

**SCHEME 1**

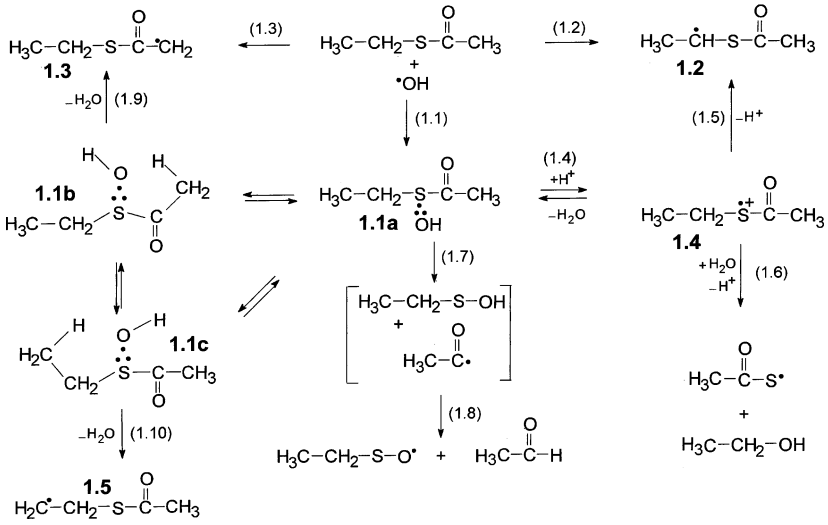

(Scheme 1, reaction 1.6) takes place as well. However, in light of a very fast deprotonation reaction (Scheme 1, reaction 1.5), the fragmentation reaction (Scheme 1, reaction 1.6) is rather of minor importance.

At very low proton concentrations, in principle, **1.1a** radicals should be stable enough to observe on the submicrosecond time scale. However, at neutral pH, no characteristic band with $\lambda_{max}$ = 340 nm, which could be assigned to such species, was observed. This observation is in line with the earlier observation in SNACET solutions.[34] Therefore, a reasonable rationale for the short-lived **1.1a** radical could be a similar fragmentation process suggesting a SNACET-derived hydroxysulfuranyl radical and involving sulfur−carbon cleavage (Scheme 1, reaction 1.7). This fragmentation process leads to the formation of acyl radicals and sulfenic acid followed by the formation of fairly stable sulfinyl radicals (RSO$^\bullet$) and acetaldehyde (Scheme 1, reaction 1.8). However, it should be pointed out that acetaldehyde was produced with a very low radiation chemical yield ($G$ < 0.1). In general, acyl radicals may also undergo an efficient fragmentation that leads to methyl radicals and CO. The lack of CO in $\gamma$-irradiated SETAc solutions points out that this reaction does not occur at all. Therefore, there must be another reaction pathway that can drastically shorten the lifetime of **1.1a** and thus prevent its observation. A mechanistically attractive and reasonable rationale for the short-lived **1.1a** is its decomposition via the elimination of water formed through a rapid intramolecular hydrogen transfer from the methyl groups. The hydrogen transfer will benefit from particularly favorable five-membered structures of **1.1b and 1.1c** that might form via the conformational rearangement of **1.1a**. These short-lived adducts should have quasi-equal delocalization of the spin density between S and O atoms, as has been noted for DMS and SETA adducts (vide supra). Moreover, hydrogen transfer that leads to the formation of alkyl-substituted radicals **1.3** (Scheme 1, reaction 1.9) should be facilitated by a low C−H bond dissociation energy. Indeed, the calculated formation energy for **1.3** (see Table 2S in Supporting Information) indicates that the C−H bond-dissociation energy in the methyl group adjacent to the carbonyl group has to be substantially lower in comparison to the C−H bond-dissociation energy in the methyl group adjacent to the methylene group. Such intramolecular hydrogen transfer within spatially close arrangements has been shown to proceed quickly. For example, hydrogen transfer from the adjacent hydroxyl groups within a six-membered structure in (alkylthio)ethanol derivatives occurred at rates of $6.3 \times 10^7$ and $1.2 \times 10^8$ s$^{-1}$ for 2-(methylthio)ethanol and 2,2′-dihydroxydiethyl sulfide, respectively.[9,14] A comparison of the formation energies of **1.3** and **1.5** radicals (Table 2S in Supporting Information) shows that the contribution of reaction 1.10 that leads to **1.5** would be rather small in the overall decomposition of **1.1a**.

**$^\bullet$OH-Induced Oxidation Mechanism of SETA.** The following observations have to be considered in the elaboration of the mechanism of the $^\bullet$OH-induced oxidation of SETA: (i) oxidation at low SETA concentration (1 mM) results in a low yield of intermolecularly three-electron-bonded dimeric sulfur radical cations SETA(>S∴S<)$^+$, both at high (0.1 M) and low ($10^{-6}$ M) proton concentrations; (ii) oxidation at high SETA concentration (>25 mM) results in a high yield of intermolecularly three-electron-bonded dimeric sulfur radical cations SETA(>S∴S<)$^+$ at high proton concentrations and in a low yield of SETA(>S∴S<)$^+$ at low proton concentration ($10^{-6}$ M); (iii) low yields of intermolecularly three-electron-bonded dimeric sulfur radical cations SETA(>S∴S<)$^+$ are always accompanied with high yields of α-(alkylthio)alkyl radicals $H_3C-CH_2-S-CH^\bullet-C(=O)-CH_3$; and (iv) oxidation at low pH results in higher yields of α-(alkylthio)alkyl radicals, $H_3C-CH_2-S-CH^\bullet-C(=O)-CH_3$, (as normalized to the actual yield of $^\bullet$OH radical concentration).

The first step in the reaction of hydroxyl radicals with SETA is an addition to the sulfur atom (Scheme 2, reaction 2.1) and the abstraction of hydrogen atoms from the methylene group located between thioether and carbonyl groups (Scheme 2, reaction 2.2), leading to the formation of hydroxysulfuranyl-type radicals (**2.1a**) and α-(alkylthio)alkyl radicals (**2.2**), respectively. At high proton concentration, the initially formed **2.1a** radicals undergo a very fast proton-catalyzed elimination of hydroxide ions (Scheme 2, reaction 2.3), generating the monomeric sulfur radical cation (**2.3**) and subsequently its dimeric form via association with the SETA molecule (**2.4**) (Scheme 2, reaction 2.4) or irreversibly deprotonate to the α-(alkylthio)alkyl radicals (**2.2** and **2.6**) (Scheme 2, reactions 2.5a andb, respectively). The observation of α-(alkylthio)alkyl radicals (**2.2**) characterized by an optical absorption spectrum with $\lambda_{max}$ = 380 nm suggests that even at low pH and high SETA concentrations (25 mM) reaction 2.5a (Scheme 2) can sufficiently compete with reaction 2.4 (Scheme 2). However, the existence of α-(alkylthio)alkyl radicals (**2.6**) has been confirmed indirectly. Time-resolved ESR (TR-ESR) experiments

**SCHEME 2**

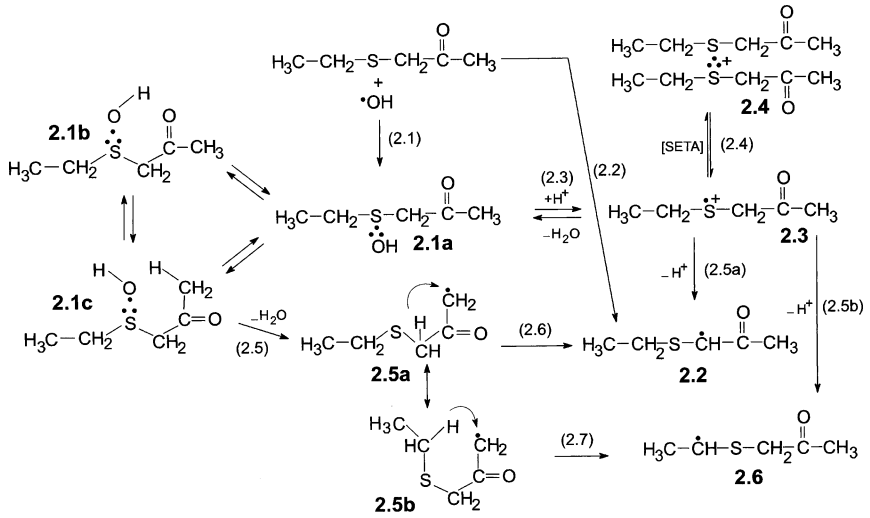

reveal the existence of acetone-derived radicals ($^{\bullet}CH_2-C(=O)-CH_3$) that are formed by the $\beta$ fragmentation of **2.6**.[65]

At low proton concentration, decomposition of the hydroxysulfuranyl radical (**2.1a**) can occur in principle via (i) a unimolecular dissociation that generates the monomeric sulfur radical cation (**2.3**) (reaction 21):

$$\text{SETA}(>S^{\bullet}-OH) \rightarrow \mathbf{2.3} + OH^- \qquad (21)$$

which subsequently associates with a SETA molecule (Scheme 2, reaction 2.4) or (ii) a displacement of $OH^-$ by a SETA molecule directly leading to **2.4** (reaction 22):

$$\text{SETA}(>S^{\bullet}-OH) + \text{SETA} \rightarrow \mathbf{2.4} + OH^- \qquad (22)$$

The lack of any significant yield of **2.4** even at high SETA concentrations (25 mM) eliminates reactions 21 and 22 as possible decay routes for **2.1a**. Now, the question is how **2.1a** radicals decay, exclusively forming α-(alkylthio)alkyl radicals. As discussed previously for the oxidation of SETAc (vide supra), the remaining alternative is the decomposition of **2.1a** via the elimination of water formed through a rapid intramolecular hydrogen transfer from the methyl groups. Moreover, it has to be pointed out that the adduct has quasi-equal delocalization of the spin density between S and O atoms (vide supra*)*. The hydrogen transfer will benefit from a particularly favorable six-membered structure of **2.1c** that is formed via the conformational rearangement of **2.1a**. Moreover, hydrogen transfer that leads to the formation of alkyl-substituted radicals **2.5a** (Scheme 2, reaction 2.5) should again be facilitated by a low C−H bond-dissociation energy. Indeed, the formation energy calculated for **2.5a** (Table 3S in Supporting Information) indicates that the C−H bond-dissociation energy in the methyl group adjacent to the carbonyl group has to be substantially lower in comparison to the C−H bond dissociation energy in the methyl group adjacent to the methylene group. Alkyl-substituted radicals **2.5a** might further be transformed into α-(alkylthio)alkyl radicals (**2.2**). It is proposed that such a transformation might involve a 1,3-hydrogen shift (Scheme 2, reaction 2.6).

Because the normalized yields (vide supra) of **2.2** radicals are substantially lower than those measured in the solutions with high proton concentration, this might suggest that the rearranged alkyl-substituted radicals (**2.5a** → **2.5b**) may still undergo another transformation. An intramolecular hydrogen transfer from the methylene group might proceed, again via a six-membered transition state (Scheme 2, reaction 2.7), leading to the α-(alkylthio)alkyl radicals (**2.6**). Similar to the solutions with high proton concentration, the existence of **2.6** radicals has been confirmed by TR-ESR experiments. They reveal the existence of acetone-derived radicals ($^{\bullet}CH_2-C(=O)-CH_3$) that are formed by the $\beta$ fragmentation of **2.6**.[65] By making a reasonable assumption that **2.6** radicals do not contribute to the 380-nm absorption band, the existence of this pathway is further corrobarated by the higher ratio of radiation chemical yields (expressed as $G \times \epsilon_{285}/G \times \epsilon_{380}$) observed in solutions at low proton concentration.

**$^{\bullet}$OH-Induced Oxidation Mechanism of SETA (Potential Involvement of Enol and Hydrate Forms).** Generally, aldehydes and ketones exist in solution as equilibrium mixtures of two isomeric forms, the keto form and the enol form (reaction A.1, Scheme 1S in Supporting Information).[66] For aliphatic ketones, there is very little of the enol present; however, we cannot discard the involvement of enols formed in the $^{\bullet}$OH-induced oxidation mechanism of SETAc. On the basis of the earlier established $^{\bullet}$OH-induced oxidation mechanisms for substituted thioethers,[14] the following reaction scheme could be developed if the *S*-ethylthioacetone enol form would be involved. The initially formed hydroxysulfuranyl radicals formed in reaction A.2 (Scheme 1S in Supporting Information) may decompose via rapid interamolecular hydrogen transfer from the adjacent hydroxyl group via the elimination of water involving the six-membered transition state (reaction A.3, Scheme 1S in Supporting Information). Hydrogen transfer leads to the formation of a highly reactive alkoxyl radical that has two possibilities to react. First, a $\beta$ cleavage of alkoxyl radicals proceeds (reaction A.4, Scheme 1S in Supporting Information), which is especially fast in polar solvents,[67] leading to α-(alkylthio)alkyl radicals and a ketene. The ketene would subequently suffer hydrolysis (reaction A.5, Scheme 1S in Supporting Information) that would eventually produce acetic acid. The alkoxyl radicals can decay competitively by an intramolecular hydrogen transfer from the $C_\alpha-H$ bond via a six-membered transition state (existed in equilibrium A.6, Scheme 1S in Supporting Information), leading to α-(alkylthio)alkyl radicals in the enol form (reaction A.7, Scheme 1S in Supporting Information) and the keto form (reaction A.8, Scheme 1S in Supporting Information). Because the $\gamma$ irradiation of near-neutral SETA aqueous solutions did not show any formation of acetate ions, the involvement of the A.4 and A.5 reactions (Scheme 1S in Supporting Information) seems to be negligible.

Aldehydes and ketones react with water to give an equilibrium

concentration of the hydrate, a gem diol (reaction A9, Scheme 2S in Supporting Information).[66] The initially formed hydroxysulfuranyl radicals formed in reaction A.10 (Scheme 2S in Supporting Information) may similarly decompose via rapid intramolecular hydrogen transfer from the adjacent hydroxyl group via the elimination of water involving the six-membered transition state (reaction A.11, Scheme 2S in Supporting Information). Hydrogen transfer leads to the formation of a highly reactive alkoxyl radical that has two possibilities to react. First, a fast $\beta$ cleavage of alkoxyl radicals proceeds (reaction A.12, Scheme 2S in Supporting Information), leading directly to α-(alkylthio)alkyl radicals and acetic acid. The alkoxyl radicals can decay competitively by an intramolecular hydrogen transfer from the $C_\alpha-H$ bond via a six-membered transition state (existing in equilibrium A.13, Scheme 2S in Supporting Information), leading to α-(alkylthio)alkyl radicals in the *gem* diol form (reaction A.14, Scheme 2S in Supporting Information) that subsequently could eliminate a water molecule (reaction A.15, Scheme 2S in Supporting Information). Again, the lack of acetate ions in $\gamma$-irradiated near-neutral SETA aqueous solutions suggests that the involvement of the A.12 reaction (Scheme 2S in Supporting Information) seems to be negligible.

## Conclusions

This paper demonstrates that the mutual location of thioether and acetyl groups affects the ultimate course of the sulfide oxidation. The results from this study show that the α-positioned acetyl group in SETAc destabilizes hydroxysulfuranyl radicals within the five-membered structure that leads to the formation of alkyl-substituted radicals. The efficacy of that process depends on the extent to which hydroxysulfuranyl radicals undergo hydroxide elimination by external proton catalysis, leading to the formation of monomeric sulfur radical cations. The latter species decay very fast via deprotonation, producing α-((alkylthio)alkyl radicals and thus preventing the formation of intermolecularly three-electron bonded dimeric radical cations even at high concentration of SETAc. A somewhat different picture is observed for SETA, which contains a $\beta$-positioned acetyl group. The main pathway involves the formation of hydroxysulfuranyl radicals and α-((alkylthio)alkyl radicals of the type $D-{}^{\bullet}CH-A$, in which D denotes an electron- donating substituent (the thioether group) and A denotes an electron-accepting substituent (the carbonyl group). The latter radicals are highly stabilized through the combined effect of both substituents in terms of the captodative effect.[68,69] Subsequently, at low pH, hydroxysulfuranyl radicals convert into intermolecularly three-electron-bonded dimeric radical cations. In contrast, at low proton concentration, hydroxysulfuranyl radicals decompose via the elimination of water, formed through intramolecular hydrogen transfer within the six-membered structure that leads to the formation of C-centered radicals. The latter radicals undergo a 1,3-hydrogen shift as well as intramolecular hydrogen abstraction leading to the α-((alkylthio)-alkyl radicals.

**Acknowledgment.** The work described herein was partially supported by the Program of the Scientific and Technological Collaboration between Poland and France POLONIUM 2000 no. 01575RD. We thank the Institut du Development et des Ressources en Informatique Scientifique (IDRIS) for providing computer facilities and technical assistance for this work (project no. 020946). We thank Gabriel Kciuk (M.Sc.) and Dr. Didier Buisson for help with acetaldehyde and acetic acid measurements and Mme Maryse Jaouen for help with CO measurements. We are deeply indebted to Dr. G. L. Hug (Notre Dame Radiation Laboratory) for supportive discussion and the careful reading of the manuscript.

**Supporting Information Available:** Radiation chemical yields expressed as $G \times \epsilon_{420}$ as a function of the concentration of SETAc , formation energies, optical absorption peaks and dipole oscillator strengths in transients from *S*-methylthioacetate and *S*-ethylthioacetone, and reaction schemes. This material is available free of charge via the Internet at http://pubs.acs.org.

## References and Notes

(1) Glass, R. S. Neighbouring Group Participation: General Principles and Application to Sulfur-Centered Reactive Species. In *Sulfur-Centered Reactive Intermediates in Chemistry and Biology*; Chatgilialoglu, C., Asmus, K.-D., Eds; Plenum Press: New York, 1990; Vol. 97, p 213.

(2) Capon, B.; McManus, S. P. *Neighboring Group Participation*; Plenum Press: New York, 1976; Vol. 1.

(3) Asmus, K.-D. Heteroatom-Centered Free Radicals: Some Selected Contributions by Radiation Chemistry. In *Radiation Chemistry: Present Status and Future Prospects*; Jonah, C., Rao, B. S. M., Eds.; Elsevier: Amsterdam, 2001.

(4) Asmus, K.-D. *Nukleonika* **2000**, *45*, 3−10.

(5) Asmus, K.-D.; Bonifačić, M. Sulfur-Centered Reactive Intermediates as Studied by Radiation Chemical and Complementary Techniques. In *S-Centered Radicals*; Alfassi, Z. B., Ed.; John Wiley & Sons: Chichester, U.K., 1999; pp 141−191.

(6) Glass, R. S.; Hojjatie, M.; Petsom, A.; Wilson, G. S.; Göbl, M.; Mahling, S.; Asmus, K.-D. *Phosphorus Sulfur Relat. Elem.* **1985**, *23*, 143−168.

(7) Schöneich, C.; Pogocki, D.; Wisniowski, P.; Hug, G. L.; Bobrowski, K. *J. Am. Chem. Soc.* **2000**, *122*, 10224−10225.

(8) Gawandi, V. B.; Mohan, H.; Mittal, J. P. *J. Phys. Chem. A* **2000**, *104*, 11877−11884.

(9) Bobrowski, K.; Hug, G. L.; Marciniak, B.; Schöneich, C.; Wiśniowski, P. *Res. Chem. Intermed.* **1999**, *25*, 285−297.

(10) Gawandi, V. B.; Mohan, H.; Mittal, J. P. *Phys. Chem. Chem. Phys.* **1999**, *1*, 1919−1926.

(11) Gawandi, V. B.; Mohan, H.; Mittal, J. P. *J. Chem. Soc., Perkin Trans. 2* **1999**, 1425−1432.

(12) Bobrowski, K.; Pogocki, D.; Schöneich, C. *J. Phys. Chem. A* **1998**, *102*, 10512−10521.

(13) Schöneich, C.; Zhao, F.; Madden, K. P.; Bobrowski, K. *J. Am. Chem. Soc.* **1994**, *116*, 4641−4652.

(14) Schöneich, C.; Bobrowski, K. *J. Am. Chem. Soc.* **1993**, *115*, 6538−6547.

(15) Bobrowski, K.; Pogocki, D.; Schöneich, C. *J. Phys. Chem.* **1993**, *97*, 13677−13684.

(16) Bobrowski, K.; Schöneich, C. *J. Chem. Soc., Chem. Commun.* **1993**, 795−797.

(17) Mohan, H.; Mittal, J. P. *J. Chem. Soc., Perkin Trans. 2* **1992**, 207−212.

(18) Bobrowski, K.; Schöneich, C.; Holcman, J.; Asmus, K.-D. *J. Chem. Soc., Perkin Trans. 2* **1991**, 975−980.

(19) Bobrowski, K.; Schöneich, C.; Holcman, J.; Asmus, K.-D. *J. Chem. Soc., Perkin Trans. 2* **1991**, 353−362.

(20) Steffen, L. K.; Glass, R. S.; Sabahi, M.; Wilson, G. S.; Schöneich, C.; Mahling, S.; Asmus, K.-D. *J. Am. Chem. Soc.* **1991**, *113*, 2141−2145.

(21) Mohan, H.; Mittal, J. P. *Radiat. Phys. Chem.* **1991**, *38*, 45−50.

(22) Bobrowski, K.; Wierzchowski, K. L.; Holcman, J.; Ciurak, M. *Int. J. Radiat. Biol.* **1990**, *57*, 919−932.

(23) Mohan, H.; Moorthy, P. N. *J. Chem. Soc., Perkin Trans. 2* **1990**, 413−416.

(24) Mohan, H. *J. Chem. Soc., Perkin Trans. 2* **1990**, 1821−1824.

(25) Asmus, K.-D. Sulfur-Centered Three-Electron Bonded Radical Species. In *Sulfur-Centered Reactive Intermediates in Chemistry and Biology*; Chatgilialoglu, C., Asmus, K.-D., Eds.; Plenum Press: New York, 1990; Vol. 197, pp 155−172.

(26) Bobrowski, K.; Holcman, J. *J. Phys. Chem.* **1989**, *93*, 6381−6387.

(27) Asmus, K.-D.; Göbl, M.; Hiller, K.-O.; Mahling, S.; Mönig, J. *J. Chem. Soc., Perkin Trans. 2* **1985**, 641−646.

(28) Hiller, K.-O.; Masloch, B.; Göbl, M.; Asmus, K.-D. *J. Am. Chem. Soc.* **1981**, *103*, 2734−2743.

(29) Schöneich, C. *Exp. Gerontol.* **1999**, *34*, 19−34.

(30) Stadtman, E. R. *Free Radical Mediated Oxidation of Proteins*; Ozben, T., Ed.; Plenum Press: New York, 1998; Vol. 296, pp 51−64.

(31) Levine, R. L.; Berlett, B. S.; Moskovitz, J.; Mosoni, L.; Stadtman, E. L. *Mech. Aging Dev.* **1999**, *107*, 323−332.

(32) Levine, R. L.; Mosoni, L.; Berlett, B. S.; Stadtman, E. R. *Proc. Natl. Acad. Sci. U.S.A.* **1996**, *93*, 15036−15040.

(33) Schöneich, C.; Zhao, F.; Yang, J.; Miller, B. *Mechanisms of Methionine Oxidation in Peptides*; Shahrokh, Z., Sluzky, V., Cleland, J. L., Shire, S. J., Randolph, T. W., Eds.; American Chemical Society: Washington, DC, 1997; Vol. 675, pp 79−89.

(34) Varmenot, N.; Remita, S.; Abedinzadeh, Z.; Wisniowski, P.; Strzelczak, G.; Bobrowski, K. *J. Phys. Chem. A* **2001**, *105*, 6867−6875.

(35) Ogino, K.; Fujihara, H. *Biochemical Reactions Involving Thioesters*; Oae, S., Okuyama, T., Eds.; CRC Press: Boca Raton, FL, 1998; pp 71−136.

(36) Ellman, G. L. A. *Arch. Biochem. Biophys.* **1959**, *82*, 70−77.

(37) Karolczak, S.; Hodyr, K.; Polowinski, M. *Radiat. Phys. Chem.* **1992**, *39*, 1.

(38) Karolczak, S.; Hodyr, K.; Lubis, R.; Kroh, J. *J. Radioanal. Nucl. Chem.* **1986**, *101*, 177.

(39) Schuler, R. H.; Patterson, L. K.; Janata, E. *J. Phys. Chem.* **1980**, *84*, 2088.

(40) Kobayashi, K.; Tanaka, M.; Kawai, S. *J. Chromatogr.* **1980**, *187*, 413−417.

(41) Antonini, E.; Brunori, M. *The Derivatives of Ferrous Hemoglobin and Myoglobin*; North-Holland: Amsterdam, 1971; Vol. 21.

(42) Rauk, A.; Armstrong, D. A.; Berges, J. *Can. J. Chem.* **2001**, *79*, 405−417.

(43) Vreck, I. V.; Siehl, H.-U. *J. Phys. Chem. A* **2002**, *106*, 1604−1611.

(44) Carmichael, I. *Nukleonika* **2000**, *45*, 11−17.

(45) Braida, B.; Hiberty, P. C.; Savin, A. J. *J. Phys. Chem. A* **1998**, *102*, 7872−7877.

(46) Li, X.; Cai, Z.; Sevilla, M. D. *J. Phys. Chem. A* **2002**, *106*, 1596−1603.

(47) McKee, M. L. *J. Phys. Chem.* **1993**, *97*, 10971−10976.

(48) Cossi, M.; Barone, V.; Menucci, B.; Tomasi, J. *Chem. Phys. Lett.* **1998**, *286*, 253−260.

(49) Cossi, M.; Adamo, C.; Barone, V. *Chem. Phys. Lett.* **1998**, *297*, 1−7.

(50) Jolibois, F.; Cadet, J.; Grand, A.; Subra, R.; Rega, N.; Barone, V. *J. Am. Chem. Soc.* **1998**, *120*, 6706−6712.

(51) Schuurmann, G.; Cossi, M.; Barone, V.; Tomasi, J. *J. Phys. Chem. A* **1998**, *102*, 6706−6712.

(52) Lhiaubet, V.; Gutierrez, F.; Penaud-Berruyer, F.; Amouyal, E.; Daudey, J.-P.; Poteau, R.; Chouini-Lalanne, N.; Paillous, N. *New J. Chem.* **2000**, *24*, 403−410.

(53) Frisch, M. J.; Trucks, G. W.; Schlegel, H. B.; Scuseria, G. E.; Robb, M. A.; Cheeseman, J. R.; Zakrzewski, V. G.; Montgomery, J. A., Jr.; Stratmann, R. E.; Burant, J. C.; Dapprich, S.; Millam, J. M.; Daniels, A. D.; Kudin, K. N.; Strain, M. C.; Farkas, O.; Tomasi, J.; Barone, V.; Cossi, M.; Cammi, R.; Mennucci, B.; Pomelli, C.; Adamo, C.; Clifford, S.; Ochterski, J.; Petersson, G. A.; Ayala, P. Y.; Cui, Q.; Morokuma, K.; Malick, D. K.; Rabuck, A. D.; Raghavachari, K.; Foresman, J. B.; Cioslowski, J.; Ortiz, J. V.; Stefanov, B. B.; Liu, G.; Liashenko, A.; Piskorz, P.; Komaromi, I.; Gomperts, R.; Martin, R. L.; Fox, D. J.; Keith, T.; Al-Laham, M. A.; Peng, C. Y.; Nanayakkara, A.; Gonzalez, C.; Challacombe, M.; Gill, P. M. W.; Johnson, B. G.; Chen, W.; Wong, M. W.; Andres, J. L.; Head-Gordon, M.; Replogle, E. S.; Pople, J. A. *Gaussian 98*, revision A.7; Gaussian, Inc.: Pittsburgh, PA, 1998.

(54) Schuler, R. H.; Hartzell, A. L.; Behar, B. *J. Phys. Chem.* **1981**, *85*, 192−199.

(55) von Sonntag, C.; Schuchmann, H.-P. *Peroxyl Radicals in Aqueous Solutions*; Alfassi, Z. B., Ed.; John Wiley & Sons: Chichester, U.K., 1997; pp 173−234.

(56) Zhang, X.; Zgang, N.; Schuchmann, H.-P.; von Sonntag, C. *J. Phys. Chem.* **1994**, *98*, 6541−6547.

(57) Tamba, M.; Simone, G.; Quintilani, M. *Int. J. Radiat. Biol.* **1986**, *50*, 595−600.

(58) Jayson, G. G.; Stirling, D. A.; Swallow, A. J. *Int. J. Radiat. Biol.* **1971**, *19*, 143−156.

(59) Buxton, G. V.; Greenstock, C. L.; Helman, W. P.; Ross, A. B. *J. Phys. Chem. Ref. Data* **1988**, *17*, 513−886.

(60) Varmenot, N.; Bergès, J.; Scemama, A.; Abedinzadeh, Z.; Bobrowski, K., to be submitted for publication.

(61) Braida, B.; Hazebroucq, S.; Hiberty, P. C. *J. Am. Chem. Soc.* **2002**, *124*, 2371−2378.

(62) Bonifačić, M.; Möckel, H.; Bahnemann, D.; Asmus, K.-D. *J. Chem. Soc., Perkin Trans. 2* **1975**, 675−685.

(63) Fourré, I.; Bergeès, J. *J. Phys. Chem. A* **2004**, *108*, 898−906.

(64) McKee, M. L. *J. Phys. Chem. A* **2003**, *107*, 6819−6827.

(65) Wisniowski, P.; Filipiak, P.; Bobrowski, K.; Hug, G. L., to be submitted for publication.

(66) Streitwieser, A.; Heathcock, C. H.; Kosower, E. M. *Introduction to Organic Chemistry*; Prentice Hall: Upper Saddle River, NJ, 1992.

(67) Avilla, D. V.; Brown, C. E.; Ingold, K. U.; Lusztyk, J. *J. Am. Chem. Soc.* **1993**, *115*, 446−470.

(68) Bordwell, F. G.; Zhang, X.-M.; Alnajjarr, M. S. *J. Am. Chem. Soc.* **1992**, *114*, 7623−7629.

(69) Sustmann, R.; Korth, H.-G. *Adv. Phys. Org. Chem.* **1990**, *26*, 131−178.